Ulm University Hospital

Institute of Virology
Director: Prof. Dr. med. Thomas Mertens

Comparison of M1- and M2- Monocyte Derived Macrophages (MΦ) in Early Events of Human Cytomegalovirus Infection

Dissertation

To obtain the Doctoral Degree of Medicine at the Faculty of Medicine, University of Ulm

Presented by

Franziska Radtke

Munich

2015

Dean of the Faculty: Professor Dr. Thomas Wirth

1st reviewer: Professor Dr. Thomas Mertens

2nd reviewer: Professor Dr. Frank Kirchhoff

Day doctorate awarded: 08.07.2016

To the Doctor

Contents

Abbreviations

AEC	3-amino-9-ethylcarbazole
AIDS	Acquired Immune Deficiency Syndrome
APN	aminoproteinase N
AP	assembly protein
APC	allophycocyanin
Aqua a.i.	Aqua ad injectabilia
BSA	bovine serum albumin
bp	base pairs
BST2	Bone marrow stromal antigen 2
CARD	caspase recruiting domain
CD	cluster of differentiation
cDNA	complementary DNA
CSF	colony-stimulating factor
CTL	cytotoxic T-cell
DE	delayed-early gene expression phases
DNA	desoxyribonucleic acid
EDTA	ethylene diamine tetraacetic acid
EGFR	epidermal growth factor receptor
ERGIC	endoplasmatic reticulum and golgi apparatus intermediate compartment
ER	endoplasmatic reticulum
FACS	fluorescence activated cell sorting
FCS	fetal calf serum
FISH	fluorescence in situ hybridization
FITC	fluorescein isothiocyanate
GM-CSF	granulocyte-macrophage colony stimulating factor
g	glycoprotein
GPI	glycosyl-phosphatidylinositol
HCMV	human cytomegalovirus
HFF	human foreskin fibroblast

HUVEC	human umbilical vein endothelial cells
IE	immediate-early gene expression phases
IFN	interferon
Ig	immunoglobulin
IL	interleukin
IL-1ra	IL-1 receptor agonist
IKK	inhibitor of κB kinase
IRF	interferon regulatory factor
LPS	lipopolysaccharide
MCP	major capsid protein
M-CSF	macrophage colony stimulating factor
MEM	minimal essential medium
MFI	mean fluorescence intensity
MHC	major histocompatibility complex
moi	multiplicity of infection
MyD88	myeloid differentiation primary response gene 88
MΦ	monocyte- derived- macrophages
ND10	nuclear domain 10
NIEP	non-infectious enveloped particles
NK	natural killer
PAMPS	pathogen-associated molecular patterns
PBMC	peripheral blood mononuclear cells
PBS	phosphate buffered saline
PCR	polymerase chain reaction
PDGFR-α	Platelet Derived Growth Factor α
PE	phycoerythrin
PFA	phosphonoformic acid
pfu	plaque forming unit
PORT	portal protein
PRR	pathogen recognition receptor
RLR	RIG-I-like receptors

RNA	ribonucleic acid
RNI	reactive nitric intermediates
ROI	reactive oxygen intermediates
rpm	rounds per minute
SCP	smallest capsid protein
siRNA	small interfering RNA
SSC	saline-sodiumcitrate
TAP	transporter of antigen presentation
TGF	tumor growth factor
TIR	Toll/IL-1 receptor
TLR	toll-like receptor
TNF	tumor necrosis factor
TRI1	minor capsid protein
TRI2	minor capsid protein binding protein
U_L	unique long genome section
UL	gene of unique long genome section
U_S	unique short genome section
US	gene of unique short genome section
VEGF	vascular endothelial growth factor

1. Introduction

1.1 Human cytomegalovirus (HCMV)

HCMV is a ubiquitous β-group herpesvirus that infects about 50 to 90% of the world population, depending on the socio-economic conditions [67].

1.1.1 Virus morphology

The main components of HCMV are (see Figure 1): the core containing the DNA (desoxyribonucleic acid) genome, the capsid, the tegument and the envelope.

Viral Genome

The viral DNA is wrapped in the viral core, a fibrillar protein structure visible by electron microscopy.

The genome of HCMV consists of 230 000 base pairs comprising at least 166 genes encoding for about 200 gene products. The DNA sequence is: one short region U_S (U for *unique*), one long region U_L and repeated sequences located at the U_S-U_L junction as well as at the terminal ends with a schematic structure *ab*-U_L-*b´a´c´*- U_S-*ca* (same letters with apostrophe representing the same gene sequences in reverse). [67]

Capsid

The viral core is surrounded by an icosahedral nucleocapsid. The capsid has a diameter of 130 nm and is composed of five main proteins: major capsid protein (MCP), a portal protein (PORT), the smallest capsid protein (SCP), a minor capsid protein (TRI1) and minor capsid protein binding protein (TRI2). In the nucleus and/ or the cytoplasm of productively infected cells three types of HCMV capsids can be found: A, B and C capsids. C capsids represent the mature capsids carrying viral DNA. A capsids merely consist of an empty capsid mantle without DNA and B capsids still contain a protein, which serves as a scaffold for the capsid proteins before DNA encapsidation, but no DNA. B capsids exist also in an enveloped form as so-called non-infectious enveloped particles (NIEP). [67]

Tegument

The tegument is a structure common to all herpesviruses. It is a proteinaceous layer placed between the capsid and the envelope.

Remarkably, most proteins of HCMV locate to this compartment, and account for roughly 40% of the virion mass. Tegument proteins are typically phosphorylated, probably to stabilize them in their localization [70]. They have a wide range of functions during the viral replication cycle [67]. Two important tegument proteins are pp65 and pp150. pp65, expressed by gene region UL83, is the most abundant component of the tegument. pp65 is detected mainly in granulocytes in the so called antigenemia assay, a diagnostic method for detection of active systemic HCMV infections in patients at risk for HCMV disease. During infection pp65 plays an important role. It contains target structures for the host's cellular immune response against the virus, but it also participates in immune evasion. [1,5,6,35,49,65,72] Worth mentioning, the non-infectious dense bodies, particles that are found during every in vitro infection, are almost entirely built by pp65.

The large matrix phosphoprotein pp150 (encoded by the gene region UL32) is associated to the nucleocapsid and, presumably through this connection, influences virion assembly and maturation [7,67,82,96].

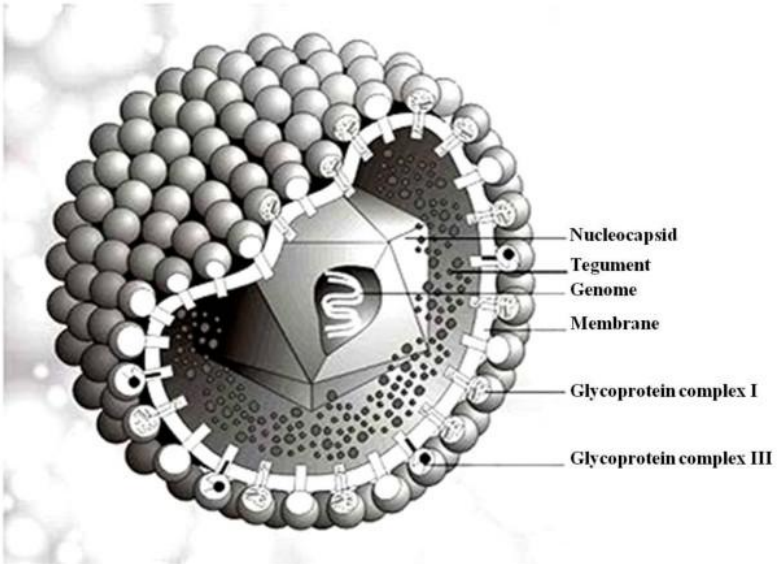

Figure 1: Structure of Human Cytomegalovirus (HCMV). (from Tomtishen III, 2012)

When tegumentation is completed in the cytoplasm, small amounts of RNA (ribonucleic acid) and cellular proteins can be included in the viral tegument [67].

Envelope

The outer virus shell is formed by the viral envelope, a lipid membrane with virus encoded incorporated glycoproteins. The better characterized glycoprotein complexes are named gB, gH:gL and gM:gN (g for glycoprotein). The two latter represent complexes of two different kinds of proteins. All these glycoproteins play a role in virus replication. [41,67] The homodimeric protein complex gB is important during attachment and entry of HCMV into cells. It binds to heparan sulfate on the cell surface to enable a stable connection [67], and may also be involved in fusion between viral and cellular membrane [43]. It has been claimed by various authors that gB also interacts with other cell surface molecules which might point to an important role during virus entry. Possible interaction partners for that are epidermal growth factor receptor (EGFR) [109], integrins [29] and Toll-like receptor 2 (TLR-2) [13]. The protein complex gM:gN binds heparan sulfate as well [67]. gH complexed with gL seems to be important in fusion, presumably via a connection to integrin alphaubeta3 [67,108]. Furthermore, gH:gL exists in multimeric complexes (e.g. including the glycoprotein gO) and heteromerics of gH:gL with the products of the genes UL128, UL130 and UL131 seem to be crucial for the cellular tropism of clinical HCMV strains in epithelial and endothelial cells. [67]

1.1.2 Viral replication cycle

Virions attach to the cell surface through connection of glycoproteins of the viral envelope with the heparan sulfate complex on the cell surface. In a second step, a more stable attachment is established, probably through interaction of the viral envelope with additional cellular receptors, which remain to be identified. [67] Virus entry into the cytoplasm takes place either as result of direct fusion between the viral envelope and the cytoplasmic membrane, e.g. in fibroblasts [67], or after endocytic uptake and subsequent fusion of the viral envelope with the vesicle membrane, e.g. in endothelial cells [67, 80]. Within the cytoplasm capsids are then transported to the nucleus using the microtubule

cytoskeleton [25]. Viral DNA and few viral proteins e.g. pp65 are introduced into the cell nucleus through the nuclear pores. Viral gene expression is divided in immediate-early (IE), delayed-early (or just "early") (DE) and late (L) phase. Start of IE expression is regulated by different viral and cellular proteins. [67] The nuclear domain 10 (ND10), a cellular structure known for its antiviral function in immune response, co-localizes with viral DNA and apparently is disintegrated in its structure and reduced in its activity during the expression of IE [27]. In fibroblasts, IE expression directly follows DNA release into the nucleus and goes on for about twelve hours. Starting from the open reading frame (ORF) UL122-UL123 four alternatively spliced messenger RNA (mRNA) can be generated, but the two most prominent are IE1 (UL123, 72 kDa) and IE2 (UL122, 86 kDa). Their products regulate subsequent viral gene expression and also influence cellular interferon-secretion (IE1) and apparently are able to block the normal cellular replication cycle (IE2) [74,111,112].

In fibroblasts, DE genes are expressed from hour 6 post cell infection (pi) till 18 to 24. Roughly, twenty DE gene products play important roles in viral DNA replication. They account for DNA synthesis and gene expression regulation, they furthermore participate in some stages of capsid maturation and they finally modify the cellular environment towards the virus' needs. Examples for DE proteins are tegument proteins pp65 and pp150 and surface glycoprotein gB (with glycosylation of the latter happening at a later point during virion maturation through cleavage of the precursor protein by a cellular protease).

It is known that once replication gets started it proceeds by a rolling cycle mechanism. Further details of the regulation of this process, also for example on the involvement of IE-proteins or ND10, are still under investigation.

Gene products are considered as L proteins when their expression starts after 24 hours pi or, according to a more strict definition, if their expression is dependent on *de novo* DNA synthesis. Proteins expressed during this L phase typically play a role in capsid construction, virus maturation and egress from the cell. For example, as DE and L gene expression proceed, a cytoplasmic reorganization takes place resulting in the formation of the assembly complex, the factory of the final maturation of the viral progeny.

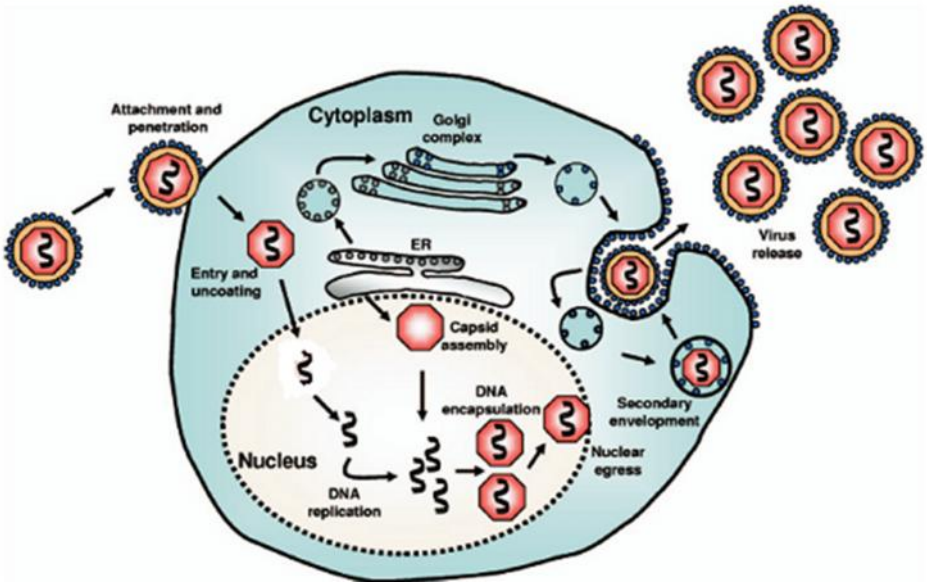

Figure 2: Human cytomegalovirus (HCMV) replication cycle. Stages of viral replication are shown starting with attachment and penetration, proceeding with entry and uncoating, translocation to the nucleus, introduction of viral DNA into the nuclear compartment, DNA replication in the nucleus, DNA encapsidation, secondary envelopment at the endoplasmatic reticulum (ER)-Golgi-intermediate compartment and egress (from Crough and Kanna, 2009).

High numbers of mature virions are released from the cell 72 to 96 hours pi. Egress most likely takes place via a three phase process: i) nucleocapsids are enveloped at the inner nuclear membrane (first envelopment), then ii) nucleocapsids are deenveloped at the outer nuclear membrane and finally iii) get enveloped again (secondary envelopment) in the cytoplasmic endoplasmatic reticulum (ER) and golgi apparatus intermediate compartment (ERGIC) prior to exocytosis. [67,75] (Figure2)

1.1.3 Pathology

HCMV can be transmitted horizontally via saliva, urine and cervical and seminal secretions as well as from mother to child transplacentally or through breast feeding.
From the entry portal at the mucosal epithelium the virus is disseminated throughout the body haematogenously, especially towards salivary glands and kidneys from where replicated virus is shed during this phase of acute infection.

Subsequently, in immunocompetent hosts, virus persists in a latent state, above all in precursor cells of the myeloid lineage, such as in monocytes and monocyte hematopoietic precursors [67]. Impairment of the physiological immune response can lead to reactivation of the latent virus [67] and monocyte-derived macrophages [92] or dendritic cells [78] have been described as site of HCMV reactivation.
In immunocompromised hosts, HCMV spreads and replicates in a wide range of organs and tissues entailing considerable morbidity [67].

1.1.4 Clinical features

Primary infection of hosts with a functional immune system is largely asymptomatic, with some cases of EBV-negative mononucleosis.
Since the control of HCMV largely depends on a functional cytotoxic T-cell (CTL) immune response, in persons with immature or dysfunctional immune response such as children in utero and immunocompromised individuals, HCMV infection can lead to severe diseases. [67]

Infection of immunocompromised patients

Solid organ and bone marrow transplant recipients as well as persons suffering from AIDS (Acquired Immune Deficiency Syndrome) are typical examples for patients with an impaired immune system. Despite the progress in terms of prophylaxis and therapy, HCMV infection in these cases can take a fatal course. Reactivation as well as primary infection can lead to severe clinical symptoms. Characteristic organs diseased during the infection are the liver and the retina, but also stomach and gut and, less common, the brain. Importantly, HCMV also can lead to severe interstitial pneumonia. After solid organ transplantation HCMV infection may lead to general illness resembling flu, grave organic disease, e.g. pneumonitis or gastroenteritis, and even transplant rejection. AIDS patients with low $CD4^+$ T-cell counts are likely to manifest CMV retinitis, gastroenteritis and other inflammatory morbidities. [67]

Congenital infection

Reactivation from latent infection or primary infection in pregnant women can lead to infection of the embryo. In up to ten percent of children infected congenitally, clinical symptoms like hepatomegaly, splenomegaly, thrombocytopenia and, as infection involves the central nervous system in about 60% of symptomatic newborns, deafness and other mental development disorders may appear. (Figure 3) The group of neonates which often react with severe symptoms to (also postnatal) infection are too early born underweight children, as their immune system often is unripe, especially concerning the adaptive immune response. [67]

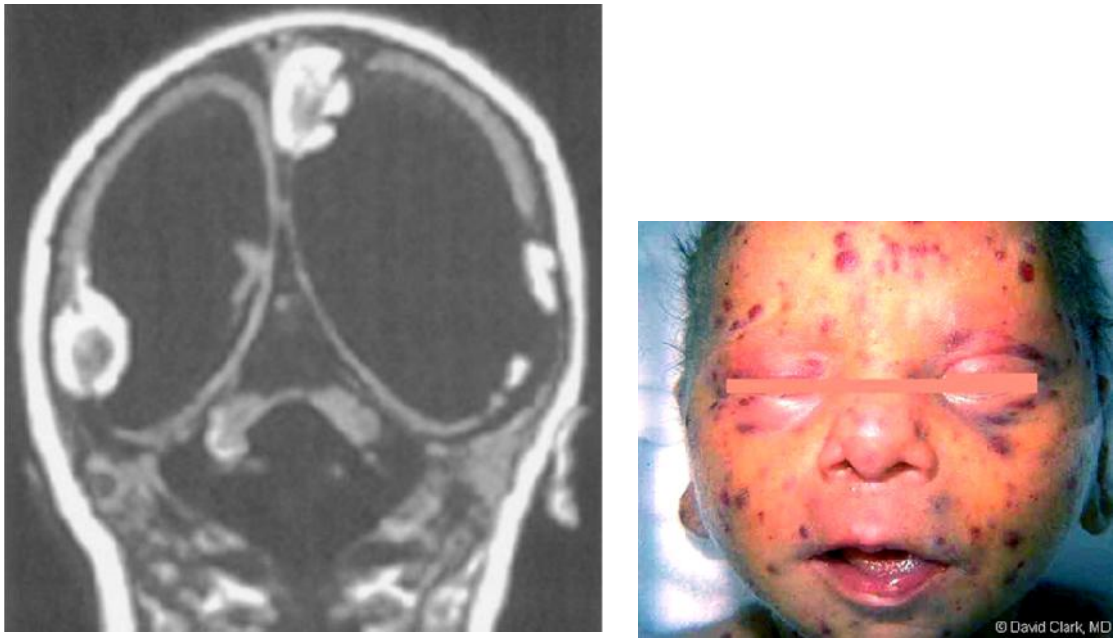

A **B**

Figure 3: Clinical features of congenital Human Cytomegalovirus (HCMV) disease. A) The coronal spin-echo shows an atrophic cerebellar structure with reduced foliation in a newborn with HCMV infection. (from Patel 2002) **B)** Child with HCMV disease showing typical “blueberry muffin”-like petechiae. (from Plosa, Esbenshade, 2012)

1.1.5 Immunoresponse and Immunevasion

Control of the infection with HCMV depends on a functional immune system. Starting from the virus' entry step into a cell, cellular gene expression reacts to infection and inflammatory cascades such as the NF-κB response are strongly activated [15,86].
As part of the early immune response, Natural Killer cells (NK) seem to curtail infection. This is suspected because various virus proteins (eg.UL16, UL140-142) are known to function as downmodulators of NK function.
Furthermore, in immunocompetent individuals, the cellular immune response, in great numbers via CTLs, urges the virus into latency and makes symptoms stop.
In addition, IgM- and IgG- antibodies, for example against surface glycoprotein gB and tegument protein pp65 (neutralising antibodies), are produced by B-cells. They limit hematogenous dissemination and provide partial protection from new infection. [67]
HCMV has developed a sophisticated and diversified strategy to overcome the human body's immune system.
pp65 [1,14], IE1 [74] and IE2 [99] among other viral proteins were shown to modify the expression and/or activation of interferon (IFN) regulated factor (IRF) -3, the secretion of host cytokines and IFNs as well as the activation of the NF-κB pathway [67].
Antigen presentation of viral components via major histocompatibility complex class I (MHC-I) as well as CTL responses are reduced by glycoproteins (gp) encoded by the viral ORF US2, US3, US6 and US11. gpUS2 and gpUS11 promote degradation of the MHCs via proteasomes, gpUS3 subverts loading with viral proteins in the endoplasmatic reticulum and gpUS6 impedes MHC-I transporting protein TAP (transporter of antigen presentation) in the ER. [67]
In order to proliferate in the host, the virus must create conditions that will allow replication during a cell's own life cycle. A viral protein stopping cell cycle at a stage preferable for HCMV (G_1/S) is pp71 [50].
Furthermore, cell death, as a component of an organism's innate defence, must be avoided by the virus to persist in the host. The IE-proteins encoded in UL37x1 and UL36 apparently prevent cellular apoptosis [77,89].

1.1.6 Diagnosis

The methods of choice to diagnose infection are detection of anti-HCMV antibodies IgG (primary infection) and IgM (reactivation) in the patient serum. Virus isolation from saliva, blood cells, cervix secretion, liquor and urine is performed inoculating the biological fluids in cultures of human cells e.g. embryonic lung fibroblasts or human foreskin fibroblasts (HFF) to cultivate HCMV *in vitro*. Observation of cytomegaly and appearance of inclusion bodies then can be found as typical cytopathic effects of HCMV. However, these phenomena can take up to a few weeks to appear. Therefore, detection of antigenemia for pp65, which is an abundant structural component of the viral particles and is expressed in infected cells 24 to 48 hours after infection, is often the detection method of choice in diagnostics.
Also, viral DNA can be measured by PCR (polymerase chain reaction)
and especially importance of the quick real time-PCR is growing. [67]

1.1.7 Antiviral treatment and prophylaxis

Antiviral drug treatment - e.g with the nucleoside analogues Ganciclovir, Valganciclovir, the DNA polymerase inhibitor Foscarnet and the nucleotide analogue Cidofovir - is reserved to immunocompromised patients or patients in life-threatening situations or newborns with impending deafness. Prophylaxis with primarily Ganciclovir is in part applied to transplant recipients. [67]

1.2 Macrophages

Macrophages are heterogeneous myeloid cells of the innate immune system [106] and are part of the mononuclear phagocyte system [103]. They free the body from cellular debris, from microbes and other immune response targets [9,16 as reviewed in 26]. The function that they are famous for since Ilya Metchnikoff is phagocytosis [95]. In addition, they are important specialized antigen recognizing and eliminating cells, they maintain and coordinate inflammation and they contribute to the adaptive immune response by stimulating T-cell functions [42].

1.2.1 Development

Macrophages represent tissue-differentiated monocytes. Monocytes are generated in the bone marrow from proliferating promonocytes and circulate in the blood stream for one to two days before infiltrating all body tissues [102]. Depending on the specific tissue micro-environment, monocytes can give rise to different macrophage subpopulations with various specializations, for example Kupffer cells in the liver, alveolar and interstitial pulmonary macrophages or microglia in the brain [9,16,26,57]. The process of tissue infiltration can be increased up to tenfold in case of tissue inflammation [103]. Additionally, recent data suggest that, at least in some settings, macrophages can proliferate locally [21].

1.2.2 Subsets

Macrophages can be polarized into different subsets [10,37,64]. The two most opposite subsets are referred to as “classically activated” and “alternatively activated” or simply as M1- and M2-macrophages. They differ significantly in secretome and immune functions. While M1 are immunogenic, pro-inflammatory cells [10], M2 appear to be more regulatory, attenuating immune defense and playing a role in tissue remodeling and wound healing [71].

M1-macrophages can kill other cells, for example by releasing reactive oxygen species and high levels of nitric oxide [38,63]. Treated with immunogenic agents e.g. LPS (lipopolysaccharide) or INF-γ they produce all kinds of pro-inflammatory substances, such as TNF (tumor necrosis factor)-α, IL-1, -6, -12 and -23 and a whole battery of chemokines [64,105]. In contrast, M2-macrophages curtail the immune response, by secreting anti-inflammatory IL-10 and IL-1ra (IL-1 receptor agonist), or promote angiogenesis inducing factors like vascular endothelial growth factor (VEGF) [8]. (see also Figure 4)

M1-macrophage secretion apparently is activated through different pathways e.g. by IRF-5 or NF-κB evoked cascades [34,55]. Conversely, in M2-macrophages different transcription factors, for example c-Maf and galectin-3 play main parts in activation

[18,61], while the NF-κB cascade seems to be shut down via the inhibitor of κB kinase (IKK) β [34].

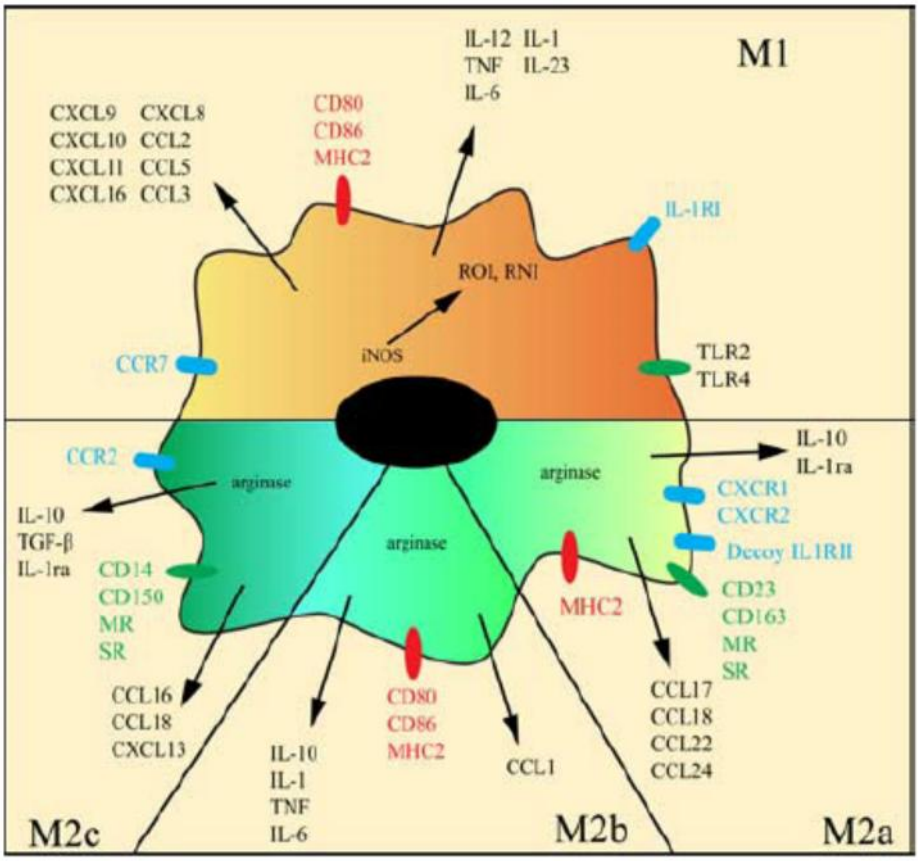

Figure 4: Subsets of macrophages. Shown are major subtypes of macrophages (M1, M2a, M2b, M2c), typical surface molecules expressed by them (CD for cluster of differentiation, MR mannose receptor, SR scavenger receptor) and chemokine ligands (CCL, CXCL), interleukins (IL) and other substances secreted by them (TLR for toll-like receptor, TGF for tumor growth factor, TNF for tumor necrosis factor, MHC for major histocompatibility complex). Also, illustrated for M1-macrophages is the production of reactive nitric (RNI) and reactive oxygen intermediates (ROI). (from Benoit 2013)

In vivo macrophage polarization is driven by environmental factors. The specific combination of extracellular cytokines and/or microbial factors can induce many more activation states than the above-mentioned M1 and M2 [10]. In a simplified view, prominent M1 polarization stimuli are INF-γ, TNF-α, GM-CSF (granulocyte-macrophage colony stimulating factor) and the bacterial LPS. M2-macrophages get polarized by exposure to IL-4 or IL (interleukin)-13 resulting in the so-called M2a or alternatively

activated macrophages. Stimulation of surface receptors such as TLRs, complement receptors or Fc receptors by immune complexes and TLR ligands leads to a slightly divergent M2 subset, named M2b, and following exposure to IL-10 and glucocorticoids M2c cells are produced [10,63,69].

In vitro M-CSF (macrophage colony stimulating factor) and GM-CSF, hematopoietic growth factors with a role in the immune response [17,40], are applied to monocytes in order to generate macrophages. These *in vitro* monocyte-derived macrophages are referred to as M1-MΦ – induced by GM-CSF - and M2-MΦ, when stimulated by M-CSF [8,105,106]. M1-MΦ are characterized by an inflammatory secretome similar to the M1-macrophages *in vivo*, including for example tumor necrosis factor and interleukins 6, 12p70 and 23, after contact with LPS. M2-MΦ are found to produce less pro-inflammatory cytokines (e.g. IL-10, chemokine ligand 2), which has also be found in the M2-macrophages *in vivo* [33,105]. They have proven to be a useful reliable model for experiments on macrophages in the past.

Nevertheless, one has to keep in mind that the classification into two subsets shows the extremes of a continuum of macrophages with varying degrees of differentiation in between [64].

1.2.3 Morphology of MΦ

M1-MΦ show a fried-egg shape and abundant cytoplasm [113]. In contrast, M2-MΦ are spindle-shaped, elongated and form an adherent monolayer in culture. Their cytoplasm is found to be filled with a huge number of vacuoles and lysosomes but only little mitochondria. By contrast, mitochondria are numerous in M1-MΦ [113]. Even if both subpopulations attach well to plastic surfaces, M1-MΦ have a higher tendency to accumulate in colonies. As to specific surface markers, CD163 has been found to be expressed in higher amount on M2- than on M1-MΦ [106,113]. Furthermore, in 2013 Wu *et al.* demonstrated that expression of TLR3, TLR7, TLR8 and cytosolic retinioid acid-inducible gene I (RIG-I) was higher in M1-MΦ than in M2-MΦ [113].

1.3 HCMV and macrophages

In vivo human macrophages are both host sentinels against virus replication on the one hand [79] and important target cells for HCMV infection on the other [88]. Macrophages may serve as a site of virus reactivation from latency [reviewed in 79,87]. Since HCMV can replicate in macrophages- though with low rates in comparison to fibroblasts [31,88] - macrophages are responsible for dissemination of the virus throughout the body [66]. Primary human M1- and M2-MΦ, representing the two types of macrophages *in vitro*, can be generated and infected in order to investigate the initial steps of HCMV infection. Strikingly, infection rates in M2-MΦ infected with the same strain of HCMV under equal conditions are found to be higher than in M1-MΦ [8]. The reason for this difference in susceptibility is so far unclear.

1.4 Putative HCMV receptors on human macrophages

It is well established that HCMV attaches to cells by binding to heparan sulfate proteoglycans on the cell surface. However, the mechanisms used to enter into the cytoplasm are not fully understood. A multitude of possible receptors and co-receptors has been proposed so far [67].

1.4.1 CD13

CD13 is a metalloproteinase also called aminoproteinase N (APN). It is expressed on the surface of epithelial cells of kidney and gut [85], on fibroblasts and on cells of the blood such as granulocytes or macrophages [60]. CD13 is known to function as peptide digestion enzyme in the gut [23] and as agent degrading neurotransmitters in the brain [60]. In the past, CD13 has been considered a binding protein for the transmissible gastroenteritis virus in pigs [24] or the human coronavirus [114]. At least two lines of evidence support a direct role of CD13 as a HCMV co-receptor [52,90,91]: firstly, HCMV binding and infection of human fibroblasts has been experimentally inhibited by using

certain monoclonal antibodies directed against CD13. Additionally, it has been shown that ectopic expression of CD13 increases susceptibility of mouse fibroblasts to HCMV [90].

1.4.2 Integrins

Integrins are heterodimeric proteins incorporated in the membranes of practically all human cells. They are important for cell adhesion to extracellular matrix or other cells but also play a role in cell signalling. Their engagement for example influences cytoskeleton architecture, gene transcription and apoptosis. Integrin receptors are composed of two peptide chains, alpha and beta. [11] In the last years integrins have been suggested as entry receptors to HCMV. The idea of their involvement in post-attachment events and fusion of the virus envelope with the cell membrane seems particularly intriguing as HCMV infection evokes a range of cellular changes characteristic of integrin-induced signalling, e.g. enhanced permeability to Ca^{2+}, induction of phospholipases C and A2, and activation of transcription factor NF-κB [54,101]. In fibroblasts, epithelial and endothelial cells integrins comprising integrin chain beta-1 were identified as possible mediators of HCMV entry. There are suggestions that a certain highly conserved domain of the virus glycoprotein gB is responsible for this interaction. This domain interestingly does not contain the RGD (arginine-glycine-aspartate) motif typical for integrin binding. Block of integrin binding as well as experiments with integrin knock-down cells showed HCMV entry is drastically reduced when the virus is not able to interact with certain integrin chains, namely beta-1 and beta-3. More specifically, integrin alphaυbeta3 has been suggested as a potential co-receptor, facilitating HCMV entry together with EGFR (see below). [29,30,108]

1.4.3 Bone marrow stromal antigen 2 (BST2)/ Tetherin

BST2 or tetherin is a protein located on the cell surface as well as in intracellular membranes of various cells [56]. Constitutive levels of expression are low on most cell types, but can be raised by stimulation with type I IFN. They are highly expressed a priori on IFN producing cells, such as plasmacytoid dendritic cells. [12] BST2 consists of 181 amino acids, with the N-terminus in the cytoplasm, a transmembrane domain, an

ectodomain exhibiting a characteristic coil-coiled structure and finally a glycosyl-phosphatidylinositol (GPI) anchor at the C-terminus [56].
Tetherin plays a role in immune defence against Kaposi Sarcoma Herpes Virus (KSHV) [62,73] and has been described as an important Human Immunodeficiency Virus (HIV) restriction factor [4,38,48,51,58,62,73,76,81,110].
Recently, and somewhat contradicting its established anti-viral role, results were found suggesting that BST2 might be an entry receptor for HCMV. Firstly, infected fibroblasts exposed to supernatants containing high amounts of BST2 showed an elevated production of IE1 as well as an increased viral genome transcription in comparison to non-treated fibroblasts.
Additionally, silencing of BST2 expression in fibroblasts and monocytes decreased viral entry and led to significantly lower levels of pp65 and IE1 after infection as well. [107]

1.4.4 EGFR

In 2003 EGFR was proposed as an entry receptor for HCMV, which supposedly functions over a connection to viral gB [109]. Breast cancer cells not expressing the receptor were transfected with complementary DNA for EGFR and new susceptibility to infection could be detected as a result. Blocking of the receptor on fibroblasts with specific antibodies led to considerable decrease in infection. The significance of the receptor for entry of HCMV into cells could be confirmed by some authors in monocytes [19], but it has been contradicted by others using similar experimental approaches [44].

1.4.5 Platelet Derived Growth Factor Receptor α (PDGFR-α)

If the expression of tyrosine kinase PDGFR-α is knocked down by siRNA (small interfering RNA) in fibroblasts, entry of HCMV as well as expression of IE1 and pp65 and synthesis of infectious progeny virus are significantly diminished. Block of the receptor binding site as well as inhibition of its signaling activity led to suppressed IE1 expression in fibroblasts, epithelial and endothelial cells.
These results argue for a role of PDGFR-α in HCMV infection, particularly as an entry receptor. There are hypotheses that viral glycoprotein gB interacts with the kinase and

triggers virus uptake. [93] Moreover, this process is thought to induce phosphorylation of the receptor entailing the activation of signaling pathways that probably are vital for long-range survival of HCMV in cells [47].
However, other results are not in agreement with this model and suggest that PDGFR-α plays a role as an inductor of unconventional entry pathways that increases HCMV infection rates, but is not necessary an entry receptor [104].

1.5 Intrinsic factors possibly influencing HCMV infection in human macrophages

Intrinsic antiviral cell factors that play a role for viral infection are TLRs, RIG-I and PML. TLRs and RIG-I are important PRRs (pathogen recognition receptors), that will sense and initiate defensive cascades against immunogenic agents like viruses. PML is a nuclear protein with antiviral features when in contact with virus DNA.

1.5.1 TLRs and RIG-I

The typical structure of TLRs roughly consists of a domain containing several leucine repeats responsible for the binding to specific pathogen-associated molecular patterns (PAMPS) and a so-called Toll/IL-1 receptor (TIR) cytoplasmic domain, giving way to intracellular downstream signaling.
The TLRs -2 and -4 are surface receptors responsible for recognition of molecules of bacterial cell walls and viruses. TLR-3 and TLR-9 by contrast are found in compartments within the cell such as the endoplasmaic reticulum or endosomes and nucleic acid species derived from viruses are recognized through them.
RIG-I is a member of a family known as RIG-I-like receptors (RLRs), RNA helicases within the cytoplasm that detect RNA species generated there. It is composed of two caspase recruiting domain (CARD)-like domains that activate downstream pathways and one RNA helicase domain.
The signaling triggered by TLR- and RIG-I activation eventually results in increased transcription of type I IFN - dependent or independently of adapter protein myeloid

differentiation primary response gene 88 (MyD88) - and other proinflammatory cytokines. [reviewed in 53]

In previous studies it has been shown that HCMV engages all of the aforementioned TLRs. Activation of TLRs 3, 4 and 9 induces inflammation and shifts cells to an antiviral state. TLR-2 interestingly also appears to be involved in early steps of infection, like attachment and virus entry [13]. But furthermore, particularly for TLR-2, reports exist showing the importance of the receptor in cellular immune response to HCMV [20]. RIG-I is increased in level of expression by activation through HCMV, leading to IFN secretion. However, 48 hours pi the virus apparently starts to counteract this effect as the destruction of the receptor is observed [84].

1.5.2 Promyelocytic leukemia protein (PML)

PML is an IFN responsive protein [94] which serves as the indispensable scaffold of a subnuclear complex called ND10 [46,115]. It has been shown that immediately upon infection, HCMV co-localizes with ND10 [2,45]. ND10 is thought to play a part in the inhibition of efficient transcription of the viral DNA [59], presumably by causing epigenetic modifications [100].

In fact, knockdown of the expression of PML in fibroblasts leads to higher replication rates of HCMV [97].

Interestingly, HCMV is able to overcome this defensive mechanism. The tegument protein pp71 counteracts the complex, which finally leads to disaggregation of the ND10 structure and unhindered expression of the first IE-gene products.

Newly synthesized IE1 then induces a complete destruction of the integrity of PML, thus permitting regular DE- and L-gene expression as well as normal viral replication rates. [22,39]

1.6 Aim of the study

In vivo macrophages can acquire a broad spectrum of functional states and the two opposite extremes have been defined as classically activated pro-inflammatory macrophages and alternatively activated anti-inflammatory macrophages. *In vitro*, cells with similar features can be generated stimulating monocytes with different growth factors and are called M1-MΦ and M2-MΦ.
HCMV, a β-herpesvirus with a high morbidity in immunosuppressed individuals, infects M2-MΦ at a higher rate than M1-MΦ *in vitro*.
This study aimed at finding out differences between M1-MΦ and M2-MΦ per se and during infection that might explain this phenomenon. Putative entry receptors (CD13, integrins, BST2/Tetherin, EGFR and PDGFR-α) as well as intrinsic cellular factors (TLRs, RIG-I, PML) were pondered as responsible agents that might influence especially the early stages of infection in the two MΦ subsets in different ways.
The investigation of these differences is interesting for several reasons.
First, finding factors that might restrict or enhance infection by comparing these cells could help to better understand the process of HCMV infection in general and what is needed on a cellular level to overcome it.
Secondly, macrophages are important immune response coordinating cells. Understanding how (different kinds of) macrophages interact with HCMV might help explain how the virus is able to persist under the defense mechanisms of the human immune system.
Finally, close examination of the differences found between the two MΦ subtypes during the HCMV infection cycle might point to characteristic differences between M1-MΦ and M2-MΦ in general. It is still not known how the two types of MΦ, differentiated from the same cell line, arrive at their antithetic phenotypes. Better comprehension is desirable as the balance of the two macrophage types, M1 and M2, plays an important role in inflammation, fibrosis and even tumor growth *in vivo*.

2. Materials and Methods

2.1 Materials

2.1.1 Chemicals, Solutions, Media and Equipment

Chemicals and Media	Company	Reference Number
3-Amino-9-ethylcarbazole	Sigma-Aldrich Chemie GmbH, Germany	A5754
Acetic acid 100% anhydrous	Merck KGaA, Germany	100063
Acetone , p.a.	Sigma-Aldrich Chemie GmbH, Germany	32201
1% Agarose (10 mg/ml) Seakem	Lonza, Switzerland	50004
Aqua ad injectabilia (Aqua a.i.)	B.Braun, Germany	2351744
Bovine serum albumine (BSA)	Sigma-Aldrich Chemie GmbH, Germany	A8327
Di-Natriumhydrogenphosphat (Na_2HPO_4)	Carl Roth GmbH & Co. KG, Germany	P030.1
Dipotassium hydrogen phosphate (K_2HPO_4)	Merck KGaA, Germany	1051041000
Dulbecco PBS (phosphate buffered saline) w/o Ca^{2+} and Mg^{2+}	PAA Laboratories GmbH, Austria	H15-002
Ethanol absolute	VWR Chemicals, France	20821.330
Ethidiumbromide solution	Carl Roth GmbH & Co. KG, Germany	2218.2

Ethylenediaminetetraacetic acid (EDTA)	Sigma-Aldrich Chemie GmbH, Germany	L2331
Fetal calf serum (FCS)	Sigma-Aldrich Chemie GmbH, Germany	F0804
37% Formaldehyde solution	Sigma-Aldrich Chemie GmbH, Germany or equivalent	252549-1L
Formamide	Sigma-Aldrich Chemie GmbH, Germany	47670-1L-F
10% Human Immunoglobulines Flebogamma	Grifols Deutschland GmbH, Langen, Germany	
Hydrogen peroxide (H_2O_2)	Fischar	6311092
L-Glutamine	PAA Laboratories GmbH, Germany	M 11-004
Lymphoprep Lymphocyte Separation Medium LSM 1077	PAA Laboratories GmbH, Germany	J15-004
Magnesium chloride 3M ($MgCl_2$)	Carl Roth GmbH, Germany	KK36.3
Methanol p.a.	Sigma-Aldrich Chemie GmbH, Germany	32213
Minimum essential medium (MEM)	Gibco life technologies, Germany	21090-022
Mixed Bed resin	Bio Rad, USA	143-7424
N,N-dimethylformamide	Merck KGaA, Germany	1.03034.1000
Paraformaldehyde (PFA)	Fluka Chemie AG, Switzerland	30525-89-4
Penicillin/ Streptomycin	PAA Laboratories GmbH, Germany	P11-010

Pepsin from gastric mucosa lyophilized powder	Sigma-Aldrich Chemie GmbH, Germany	091M7020V
Potassium hydrogen phosphate (KH_2PO_4)	Merck KGaA, Germany	1370395000
RPMI media 1640	Gibco life technologies, Germany	13870-025
Sodium acetate	Merck KGaA, Germany	1.06267.1000
Sodium azide	Sigma-Aldrich Chemie GmbH, Germany	S2002
Sodium chloride	Sigma-Aldrich Chemie GmbH, Germany	31434-IKG-R
20x SSC (saline-sodiumcitrate) Buffer (0.3 M sodium citrate in 3 M NaCl)	Sigma-Aldrich Chemie GmbH, Germany	S6639-1L
Sucrose	Sigma-Aldrich Chemie GmbH, Germany	S0389
Triton-X-100	SERVA GmbH, Germany	37238
Trypan blue	Carl Roth GmbH & Co. KG, Germany	L6323
Trypsin	PAA, Austria	L11-660

Growth factors	**Company**	**Reference Number**
Recombinant GM-CSF	R & D Systems, USA	215-GM
Recombinant M-CSF	R & D Systems, USA	216-MC

Special materials for cell preparation

Monocyte Isolation Kit	Company	Reference Number
Monocyte Isolation Kit II human	MACS Miltenyi Biotec	130-091-153

Separation Columns for Monocyte Isolation	Company
LS Columns	MACS Miltenyi Biotec

Antibodies for indirect immunofluorescence

Primary antibodies for indirect immunofluorescence	Company	Reference number	Used dilution
Purified Mouse Anti-Human CD13	BD Pharmingen, Germany	555393	pure
Mouse Anti-IE 1-2 (anti-CMV I.E.A.)	Argene, France	11-003	1:500
PML (PG-M3)	Santa Cruz Biotechnology, Inc.	sc-966	1:50
Hybridoma anti-gB 27-287	laboratory stock		pure
Hybridoma anti-pp150	laboratory stock		pure
Anti-pp65	Argene, France		1:20
Gammunex 10% Human Immunoglobulins	Talecris, Biotherapeutics	G120031	1:100

Secondary antibodies for indirect immunofluorescence	Company	Reference number	Used dilution
Alexa Fluor 488 F(ab')2 fragment of goat anti-mouse IgG (H+L)	invitrogen™ by lifetechnologies, USA	A11017 991633	1:1000
Alexa Fluor 555 F(ab')2 fragment of goat anti-mouse IgG (H+L)	invitrogen™ by lifetechnologies, USA	A21425 997829	1:1000

Antibodies for flow cytometry

Antibodies for Fluorescence Analysis Cell Sorting	Company	Reference Number	Used dilution
Purified Mouse Anti-Human CD13	BD Bioscience Pharmingen	555393	1:10
PE Mouse anti human CD14	BD, Germany	555398	1:25
PerCP Mouse IgG1 κ Isotype	BD Bioscience Pharmingen	559425	1:2
IgG2a PE Isotype control	MACs	130-098-849	1:5
Mouse IgG2b Isotype control Phycoerythrin	R & D Systems, USA	IC0041P	1:5
Polyclonal Goat Anti-Mouse Immunoglobulins/ RPE Goat F(ab')2	Dako Denmark A/S, Denmark	R0480	1:20
Mouse IgG1 control PE-conjugated	Immunotools, Germany	21275514S	1:25
Mouse IgG1 control APC-conjugated	Immunotools, Germany	21275516S	1:25

Mouse IgG2a control PE-conjugated	Immunotools, Germany	21275524S	1:25
Anti-human CD1a FITC-conjugated	Immunotools, Germany	21270013S	1:25
Anti-human CD11a APC-conjugated	Immunotools, Germany	21270116S	1:25
Anti-human CD11b PE-conjugated	Immunotools, Germany	21279114S	1:25
Anti-human CD11c APC-conjugated	Immunotools, Germany	21487116S	1:25
Anti-human CD18 PE-conjugated	Immunotools, Germany	21270184S	1:25
Anti-human/ -mouse/ -porcine CD29 FITC-conjugated	Immunotools, Germany	21270293S	1:25
Anti-human CD41a FITC-conjugated	Immunotools, Germany	21810413S	1:25
Anti-human CD49d FITC-conjugated	Immunotools, Germany	21488493S	1:25
Anti-human CD61 FITC-conjugated	Immunotools, Germany	21330613S	1:25 1:10
Anti-BST2 antibody	kindly provided by the Institute of Molecular Virology, University Hospital, Ulm		
PE Mouse Anti-Human CD14	BD Pharmingen, Germany	555398	1:25
PE Mouse Anti-Human EGF Receptor	BD Pharmingen, Germany	555997	2:5

PE Mouse Anti-human CD140a	BD Pharmingen, Germany	556002	2:5

Fixation/ Permeabilization Kit	
Cytofix/ Cytoperm™ Fixation/ Permeabilization Kit	BD Biosciences, USA

Special materials for RNA extraction, reverse transcription and PCR

RNA isolation kit	**Company**	**Reference number**
RNeasy Mini Kit 50	Roche, Switzerland	74104

PCR Reagents	**Company**	**Reference number**
100 bp DNA ladder	NEB, Germany	N32315
5x reaction buffer for M-Mul V RT	Fermentas, Lithuania	EP0451
DNAse I, RNAse free	Fermentas, Lithuania	EN0521
EDTA	Fermentas, Lithuania	
Oligo $(dT)_{18}$ Primer	Fermentas, Lithuania	SO132
PCR nucleotide mix 10 mM	Roche, Switzerland	11814362001
RiboLock RNAse Inhibitor	Fermentas, Lithuania	EO0382
RevertAid H Minus M-Mul V reverse transcriptase	Fermentas, Lithuania	EP0451
PCR reaction buffer 10x	Roche, Switzerland	11271318001
Taq DNA polymerase	Roche, Switzerland	11435094

DNA ladder	**Company**	**Reference Number**
100 bp ladder	New England Biolabs, Germany	N3231

Special materials for fluorescence in-situ hybridization (FISH)

FISH DNA Probe	**Company**	**Reference Number**
ON C-MET (7q31)/ SE 7	Kreatech Diagnostics, Netherlands	KBI-10719

Equipment

Flasks, tubes and plates	
75 cm^2 tissue culture flask (T75)	Sigma-Aldrich Laboratories GmbH, Germany
Tube 50 ml, plastic Tube 15 ml, plastic Tube 1.5 ml, plastic Tube 2 ml, plastic 5 ml Polystyrene Round-Bottom Tube	Falcon Falcon Eppendorf, Germany Eppendorf, Germany BD Falcon, Germany
96-well plate, U-bottom with lid 96-well plate, F-bottom with lid Ibidi-slide 15 µ slides, 8 wells Culture dishes lumox® dish 35	Greiner bio-one CELLSTAR® Greiner bio-one CELLSTAR® ibiTreat SARSTEDT Aktiengesellschaft, Germany

Object slides and cover glasses	
30 Menzel Gläser, cut edges, frosted end	Gerhard Menzel GmbH, Germany
100 Deckgläser 24 x 60 mm #1 Menzel Gläser	Gerhard Menzel GmbH, Germany
IMM ibidi Mounting Medium for fluorescence microscopy	Ibidi GmbH, Germany

Water bath	
37°C water bath	Kottermann Labortechnik, Germany
42°C water bath	GFL

Sterile bench	
HERA safe	Heraeus, Germany

Incubator	
HERA cell 150i CO_2 Incubator	ThermoScientific, Germany

Centrifuges	
Eppendorf centrifuge 5417C	Eppendorf, Germany
Megafuge 1.0	Heraeus, Germany
Megafuge 1.0R	Heraeus, Germany
L7-56 ultracentrifuge	Beckman, USA
Cytofuge® Cytocentrifuge Stat Spin 2	Stat Spin, USA

Heating blocks	
Thermomixer compact	Eppendorf, Germany
Thermostat 5320	Eppendorf, Germany

Vortexer	
Vortex genie 2™	Bachofer Laboratoriumsgeräte, Germany

Flow cytometer	
FACSCalibur	BD, Germany

Gel Imaging and Documentation	
Gel Doc 2000	Bio-Rad Life Science, USA

Microscopes	
Primo Vert	Zeiss, Germany
Fluorescence microscope Axiovision	Zeiss, Germany

Pipettes	
Sarstedt serological pipettes 5 ml	Sarstedt, Germany
Sarstedt serological pipettes 10 ml	Sarstedt, Germany
Sarstedt serological pipettes 25 ml	Sarstedt, Germany

2.2 Methods

2.2.1 Cell culture

Solutions and media

Table 1| Recipe: Washing Buffer

Washing Buffer	
500 ml	Dulbecco's Phosphate Buffered Saline (PBS)
10 ml	1% ethylene diamine tetraacetic acid (EDTA) in PBS w/o Ca^{2+}, Mg^{2+}

Table 2| Recipe: Miltenyi Buffer

Miltenyi Buffer	
500 ml	Dulbecco's Phosphate Buffered Saline (PBS)
10 ml	1% ethylene diamine tetraacetic acid (EDTA) in PBS w/o Ca^{2+}, Mg^{2+}
8.3 ml	30% bovine serum albumin (BSA)

Table 3| Recipe: RPMI Complete Medium 10% FCS

RPMI Complete Medium 10% FCS	
50 ml	Fetal calf serum (FCS)
5 ml	2 mM L-Glutamine
5 ml	100 U/ml Penicillin/Streptomycine
Fill up to 500 ml with	RPMI

Cell preparation

Monocytes were isolated from buffy-coats obtained from the Institut für Klinische Transfusionsmedizin und Immungenetik Ulm GmbH. The monocytes were separated from other PBMC (peripheral blood mononuclear cells) by negative selection using the MACS™ monocyte isolation kit II. Therefore 30-40 ml blood were first diluted with 50-60 ml Dulbecco's PBS. 35 ml of this dilution were carefully transferred into a tube containing 15 ml lymphoprep solution, always carefully preventing the liquids from mixing. For each buffy-coat two tubes were centrifuged at 1650 rpm (rounds per minute) for 25 minutes without brake.

The white rings which contain mononuclear cells (Figure 5) were collected and centrifuged after the addition of a washing buffer of Dulbecco´s PBS 1% EDTA (see Table 1) at 1450 rpm for 10 minutes. In order to remove all residues of the lymphoprep the pellet was washed again in the same way. To remove the platelets, the pellet was resuspended in Dulbecco's PBS 1% EDTA prior to centrifugation at 1100 rpm and 900 rpm. The thus isolated PBMC, which include monocytes, B-, T- and NK-cells besides monocytes, were counted in a Neubauer counting-chamber. 150 x 10^6 PBMC were transferred into a new tube, topped up to 30 ml with washing buffer and centrifuged at 1100 rpm for 7 minutes.
Monocytes were subsequently isolated by negative selection using MACS™ monocyte Isolation Kit II. The pellet was resuspended in 450 µl Miltenyi Buffer (see Table 2) consisting of Dulbecco's PBS 1% EDTA 8.3% BSA. 150 µl human Ig antibodies were added as a Fc-receptor blocking reagent. 150 µl of a cocktail of biotin-conjugated monoclonal antibodies against CD3, CD7, CD16, CD19, CD56, CD123 and Glycophorin A were added to the cell population. Cells then were incubated at 4 °C for 10 minutes. 450 µl Miltenyi Buffer as well as 280 µl monoclonal antibodies were added, the latter of which are conjugated to MicroBeads.

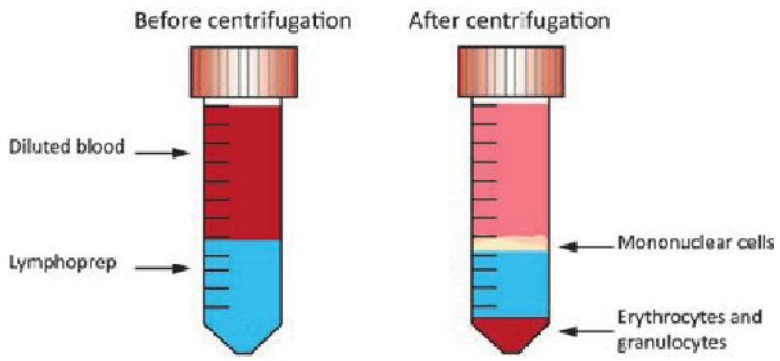

Figure 5: Buffy-coat preparation before and after centrifugation. Peripheral blood mononuclear cells are isolated from buffy-coat preparations by layering the diluted blood sample on a lymphoprep solution and a subsequent density centrifugation. Afterwards the cells can be aspirated from the interphase between the lymphoprep and the plasma. (from https://www.researchgate.net/figure/268006373_fig4_Figure-4-Separation-of-mononuclear-cells-from-blood-by-density-gradient-centrifugation)

After 15 minutes at 4 °C Miltenyi Buffer was added up to 50 ml for another centrifugation, at 1200 rpm for 10 minutes. The pellet was resuspended properly in 750 µl Miltenyi Buffer and applied to a MACS™ LS column which was attached to a MiniMACS™ isolation magnet and previously primed with Miltenyi Buffer. In this strong magnetic field labelled cells were retained inside the column because of the paramagnetic MicroBead particles attached to them and non-labelled monocytes could flow through. (Figure 6) In order to thoroughly elute all unlabelled monocytes, the column was washed three times with 3 ml Miltenyi buffer. All flow-through was collected and centrifuged at 1200 rpm for 7 minutes. The pellet was resuspended in 2 ml RPMI medium containing 10% FCS for cell counting in a Neubauer counting-chamber. Then, the monocytes were diluted in RPMI 10% FCS (see Table 3) to a final concentration of 3 x 10^6 cells per ml and 2 ml were seeded into sterile lumox® dishes.

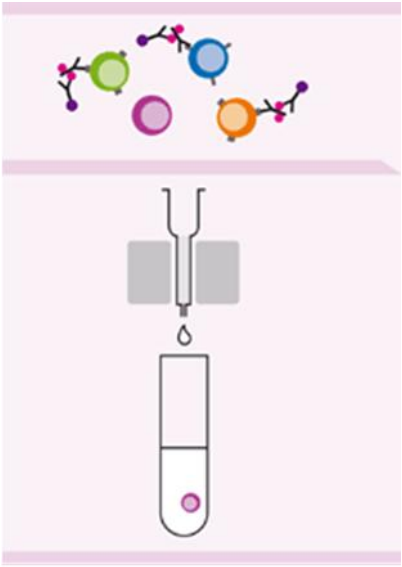

Figure 6: Monocyte isolation using MACS™ Monocyte isolation kit II.
Peripheral blood mononuclear cells (PBMC) are labeled with magnetic antibodies against surface molecules that are not present on most monocytes (depicted as purple cells). Cells subsequently are exposed to a magnetic field within a column-shaped filter. The labeled cells are retained in the column because of their magnetic antibody coating. Monocytes are not labeled and can be collected as flow-through. (modified from https://www.miltenyibiotec.com/en/products-and-services/macs-cell-separation/cell-separation-reagents/monocytes-and-macrophages/monocyte-isolation-kit-ii-human.aspx)

For differentiation of monocytes into macrophages *in vitro* (MΦ) specific growth factors were added at a concentration of 100 ng/ml: GM-CSF was used to generate M1-MΦ and M-CSF to generate M2-MΦ, respectively. Cell cultures were kept in an incubator at 37°C. After 3 days the exhausted medium was replenished: 900 µl per dish were removed and centrifuged in tubes at 1200 rpm for 7 minutes to collect floating cells. The pellet was resuspended in fresh RPMI 10% FCS and put back into the dish. Growth factors were added as at the beginning of the culture. Viable cells were continuously monitored for contamination under a light microscope and kept under sterile conditions at all times. One week after isolation monocytes had visibly differentiated into MΦ: the cells had attached to the surface, they became bigger in size and had a less round shape than monocytes. The MΦ were detached by alternating incubation in Dulbecco´s PBS for 5 minutes at 37°C and frequent pipetting and could be used for further experiments

2.2.2 Virus production

Solutions and media

Table 4| Recipe: Sucrose phosphate buffer

Sucrose phosphate buffer	
74.62 g	Sucrose
1.218 g	K_2HPO_4
0.52 g	KH_2PO_4
Fill up to 1000 ml with	aqua dest.
Filtrate sterile	

Table 5| Recipe: Staining solution

Staining solution used for plaque titration assay	
One tablet	3-amino-9-ethylcarbazole (AEC)
dissolved in 4 ml	N,N-dimethylformamide
with 16 ml	acetate buffer (pH 5) (see Table 6)
and 30 µl	H_2O_2

Table 6| Recipe: Acetate buffer

Acetate buffer	
2.05 g	Sodiumacetate
Ad 500 ml with	H_2O
pH 5 with	Acetic acid 100% anhydrous

Virus production and titration

Virus was produced under sterile conditions.

Human foreskin fibroblasts (HFF) were grown in minimal essential medium (MEM) in four 75 cm^2 tissue culture flasks (T75). When the cells were confluent, the medium was discarded and 3 ml PBS 2% EDTA were added and distributed homogeneously before discarding them again to wash off the medium. This washing step was repeated twice. Next, 1 ml trypsin solution was added to the cells and evenly distributed. Incubation with this solution for cell dissociation was performed for maximum 5 minutes at 37°C. 5 ml MEM were added and used to collect all cells by repeated rinsing. The medium with the detached fibroblasts was transferred into a 50 ml tube. 0.7-1.5 x 10^5 HCMV-infected human umbilical vein endothelial cells (HUVEC) which had been stored in liquid nitrogen, were thawed in a 37° C water bath and added drop by drop to another 50 ml tube filled up to 20 ml with MEM. Both tubes were centrifuged at 1100 rpm for 7 minutes. The pellets containing either fibroblasts or the infected HUVEC were each resuspended in 1 ml MEM. Five new T75 flasks, each containing 10 ml medium, were prepared. The HFF suspension was mixed with the resuspended infected HUVEC. The proportion of HUVEC:HFF was 1:24. The mixed cell cultures of HFF and HUVEC then were distributed equally into the T75 flasks and the virus was propagated at 37°C for several days. When cells showed cytopathic effects, such as plaque formation and nuclear inclusion bodies, the supernatants were harvested and replaced by new medium. They were stored at 4°C for two days while infected cells maintained at 37°C. At day 3 the supernatants were collected again. Then, all supernatants were centrifuged at 5000 rpm at 4°C for 10 minutes, using maximum brake. In this way, cellular debris was concentrated in the pellet. The fluid phase was distributed to pre-cooled polyallomer centrifuge tubes and balanced carefully into a SW28 rotor of a Beckman L7-65 ultracentrifuge. Ultracentrifugation took

place for 1 hour at 23 000 rpm at 4°C, stopping at maximum brake. The supernatants were discarded and the virus pellet was resuspended in 250 µl of the cryoprotectant sucrose-phosphate buffer (see Table 4) and the tubes were sealed with parafilm and shaken gently for 3 hours to overnight at 4°C. Then, the virus pellet was completely resuspended by pipetting up and down 30 to 70 times and adding an appropriate volume of a 1:1 solution of MEM and sucrose phosphate buffer (Table 4). After careful mixing the virus solution was aliquoted in sterile eppendorf tubes and stored at -80°C.
To determine the virus titer a titration assay was performed in HFF: On a 96-well plate tenfold dilutions of virus in MEM (10^{-2} to 10^{-10}) were added to MEM containing HFF of the same culture (cultured and detached as described above) 1:1. This was performed in triplicate for each dilution. The plate was kept in an incubator for 2 days at 37 °C. The medium was discarded and the wells were washed in 0.01 M PBS. Fixation and permeabilization of infected cells was performed by addition of 200 µl of methanol:acetone (1:1) to each well and subsequent incubation at -20°C for 10 minutes. Fixation solution was discarded and wells were dried.
To stain infected cell nuclei, wells were first incubated with 100 µl of PBS 1% milk for 15 minutes at 37°C to block unspecific antibody binding sites. After removal of the blocking solution, 100 µl of the hybridoma supernatant 63-27, containing antibodies against the virus antigens IE 1-2, were added to each well and incubated at 37°C for 45 minutes. Then, cells were washed with 200 µl PBS thrice prior to addition of 100 µl of a prepared staining solution (see Table 5). After 15 to 30 minutes the staining reaction was accomplished, the cells were washed and stored in PBS at 4 °C. The number of IE1-2 positive red colored nuclei per well was counted under a light microscope at a dilution with roughly 10-100 red nuclei . The virus titer (in plaque forming units pfu) was calculated using the following formula:

virus titer [pfu/ml] = dilution factor x mean number of red nuclei per well at dilution d

2.2.3 HCMV infection of MΦ

For all experiments with HCMV infection, the endotheliotropic laboratory strain TB40E was used.

Prior to infection, the frozen virus was thawed in a water bath at 37°C. The number of cells to infect was determined by counting in a Neubauer chamber under the light microscope. The needed volume of virus preparation was calculated from the virus titer and the required multiplicity of infection (moi) in the following way:

$$\text{volume of virus stock} = \frac{\text{moi x cell number}}{\text{virus titer}}$$

The moi is defined as the mean number of infectious units per cell. The calculated volume of virus stock was added to the cells in medium and kept at 37 °C until fixation of the cells at the indicated time post infection (pi) .

2.2.4 Indirect immunofluorescence

Solutions

Table 7| Recipe: Phosphate Buffered Saline (PBS)

0.01 M Phosphate Buffer Saline (PBS)	
8.5 g	NaCl
1.36 g	KH_2PO_4
Adjust pH to 7.8 using	1M HCl and 1M NaOH
fill up to 1000 ml with	aqua dest.

Table 8| Recipe: Paraformaldehyde (PFA)

4 % Paraformaldehyde (PFA)	
4 g	PFA
100 ml	0.01 M Phosphate Buffered Saline (PBS)
Dissolve in 50 ml PBS first, stir magnetically at 40°C, adjust pH to 7.2 with	1M HCl or NaOH
add residual 50 ml PBS	

Table 9| Recipe: Triton

Phosphate Buffered Saline (PBS) 0.2 % Triton	
100 ml	0.01 M PBS
200 µl	Triton X-100

Table 10| Recipe: 0.01 M Phosphate Buffered Saline (PBS) 1% Bovine Serum Albumin (BSA)

0.01 M Phosphate Buffered Saline (PBS) 1% Bovine Serum Albumin (BSA)	
50 ml	0.01 M PBS
1.7 ml	30% BSA

<u>Immunofluorescence staining</u>

Indirect immunofluorescence is a method suited for detection of cellular and viral antigens. It is based on the specific antigen recognition by a primary antibody followed by additional binding of a secondary fluorescence-labeled antibody recognizing the primary antibody. To examine MΦ using this technique, 1 x 10^5 cells were seeded into each well of ibidi-slides. After one day, the MΦ had attached to the well, the medium was removed and cells were washed with PBS (see Table 7). Fixation of the cells was performed using 4% PFA (see Table 8). PFA is a cross-linking fixative which binds cellular proteins covalently, which preserves them from degradation while maintaining the cellular structure. The cells were washed twice with PBS. The cellular membranes were permeabilized by incubation for 2 minutes with 0.2% Triton-X-100 solution (see Table 9) in order to allow intracellular antibody penetration. Subsequently, they were washed twice with PBS. 250 µl of the primary antibody dilution in 0.01 M PBS 1% BSA (see Table

10) were added per well and the cells were incubated for one hour at 37°C. Then, after washing thoroughly with PBS, 150 µl of the secondary antibody dilution were incubated on the cells for 30 minutes at 37°C. From now on, the cells were kept in the dark. Afterwards, the cells were washed three times with PBS. If indicated, the cytoplasm was visualized by 0.001% Evansblue which was added to the cells (250 µl/well) for 3 min at room temperature. The cells were stored in PBS at 4° C, protected from light, until confocal microscopy and analysis were performed using AxioVision software.

2.2.5 Flow cytometry/ Fluorescence Activated Cell Sorting (FACS)

Solutions

Table 11| Recipe: Fluorescence Activated Cell Sorting (FACS) blocking solution

Fluorescence Activated Cell Sorting (FACS) blocking solution	
1.5 ml	Fetal calf serum (FCS)
500 µl	1% NaN_3 Sodium azide
5 ml	Human Immunoglobulins
Fill up to 50 ml with	0.01 M Phosphate Buffered Saline (PBS)

Table 12| Recipe: Fluorescence Activated Cell Sorting (FACS) Washing Buffer

Fluorescence Activated Cell Sorting (FACS) Washing buffer	
15 ml	Fetal Calf Serum (FCS)
5 ml	1% NaN_3 Sodium azide
Fill up to 500 ml with	0.01 M PBS

Flow cytometry staining

A flow cytometer contains at least one laser emitting monochromatic light. The sample is injected into a sheath fluid and transported to the laser. In this way, the cells are separated so that only one cell after another passes through the laser beam. When the cells in the sample are hit by the light source, they scatter the light depending on their size and granularity.

These parameters are then sensed by a detector and can be recorded and quantified by a connected computer and suitable software. Cells which were previously stained with fluorescently labeled antibodies absorb part of the light reaching them and thereby emit light at a different wave length. In this way the amount of cells which have bound the

antibody (= percentage of positive cells) as well as the average number of antibodies which have bound per cell (= mean fluorescence intensity MFI) can be measured. To distinguish the different fluorescence intensities a complex system of lenses and filters lies between the laser beam and the detector as another component of the flow cytometer.

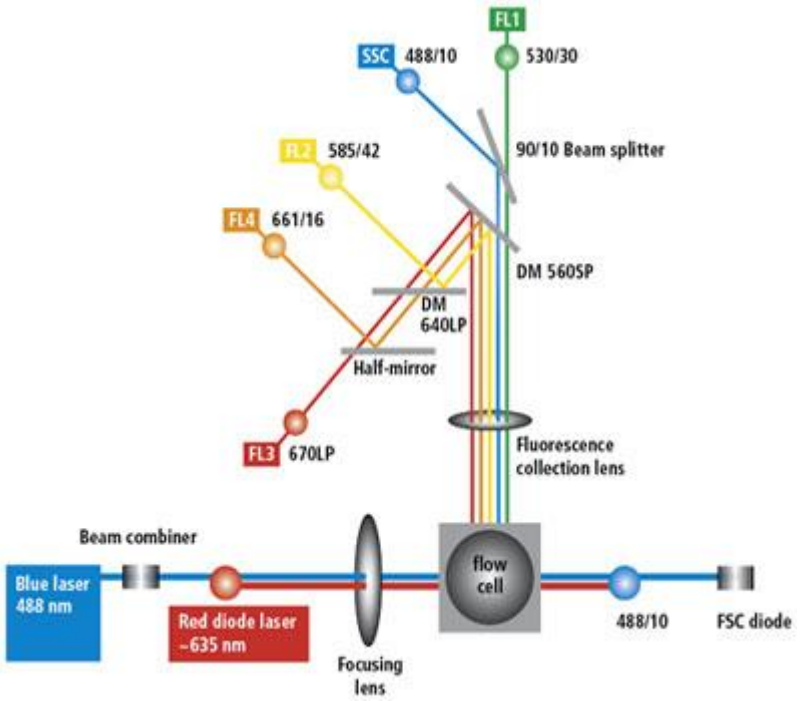

Figure 7: BD FACSCalibur optical path configuration. Fluorescently labelled cells flowing through the cytometer are exposed to laser light. The light which is emitted by the cells passes through a collecting lens and a system of mirrors (Fluorescence collecting lens, DM 560SP, 90/10 Beam splitter, DM640LP, Half mirror) and can be quantified separately in individual channels (FL1-4, depicted with the corresponding wave lengths : the first number is the mean, the second the width of the detected spectrum) depending on the respective wave length which refer to the fluorescent antibodies bound to the cells. In the SSC channel granularity is measured, in the FSC cell size.
(from http://www.bdbiosciences.com/instruments/facscalibur/features/)

To detect molecules on the surface of the cell membrane, the staining was performed in the following way. Depending on the experiment, around 1 x 10^6 cells were detached from culture dish and spun down. The pellet was resuspended in FACS blocking solution (see Table 11) and the cells were distributed into FACS tubes (50 µl per tube). Antibodies were added in the concentration recommended by the manufacturer instructions and

were incubated with the cells for one hour at 4°C in the dark. If necessary, a secondary, fluorescently labeled antibody directed against the primary antibody was added to the sample after washing with PBS FACS Washing Buffer (see Table 12) (addition of 1ml PBS followed by centrifugation 1300 rpm, 5 minutes, 4°C). The cells were resuspended in a fixation solution to render them resistant to degradation and could be stored at 4°C until acquisition.

For the analysis of differential surface and intracellular distribution of proteins, a portion of the cells was permeabilized using 1 ml BD Cytofix/Cytoperm Solution. After 20 minutes of incubation on ice, they were washed using 1 ml BD Perm/Wash buffer and after centrifugation (1300rpm, 5 minutes, 4°C) resuspended in the same buffer. At this point the cells were permeable and were incubated with the antibodies of interest and washed and fixed as described before for the surface staining.

At the BD FACSCalibur cytometer the cells stained with FITC (fluorescein isothiocyanate)-labelled antibodies were detected in channel FL-1, PE (phycoerythrin) –labeled cells in FL-2 and APC (allophycocyanin) –labeled cells in channel FL-4.

2.2.6 RNA-extraction, reverse transcription (RT) and PCR

In order to quantify expression levels of genes of interest RNA was isolated and transcribed into cDNA (complementary DNA) using reverse transcriptase. cDNA then could be used for amplification of specific gene sequences by PCR.

RNA extraction

For RNA extraction the Qiagen RNEasy Mini Kit was used according to the manufacturer instructions. Briefly, 1 x 10^6 cells were transferred into an eppendorf tube, centrifuged at 10 000 rpm for 5 minutes, and lysed by resuspending the pellet with 350 µl RLT buffer followed by vortexing. The homogenized cell lysate was mixed with 350 µl of 70% ethanol. The lysate was then transferred onto a spin column placed in a collection tube. After centrifugation for 15 seconds at 10 000 rpm, the flow-through was discarded and 700 µl of RW1 buffer were added onto the spin column before repeating the centrifugation and discard of supernatant. Next, 500 µl of RPE buffer were added onto

the spin column and centrifugation was performed for 15 seconds at 10 000 rpm. This step then was repeated, but with a centrifugation for 2 minutes at 10 000 rpm. Final centrifugation was performed at 13 000 rpm for 1 minute to remove residual buffer and then 25 µl RNAse free water were added to centrifugation for 1 more minute at 10 000 rpm to elute the RNA.

To exclude genomic DNA contamination, the RNA template was treated with DNAse I according to the manufacturer instructions. Briefly, the DNA residues in 24 µl of RNA template were digested by 3 µl DNAse I in 3 µl of 10x DNAse I buffer containing $MgCl_2$. After incubation at 37°C for 30 minutes on a heating block, 3 µl of EDTA were added – to avoid chelate formation by metal ions – and incubated for 10 minutes at 65°C and then chilled on ice.

Reverse Transcription

Fermentas RevertAid H Minus First strand cDNA Synthesis Kit was used for reverse transcription. This technique was performed with a negative control for each sample, which was not supplemented with any reverse transcriptase and hence cannot be transcribed into cDNA. In the beginning, 1 µl Oligo $(dT)_{18}$ primers was added to 11 µl RNA of each sample, in order to give a starting point for the transcriptase. After an incubation time of 5 minutes at 65°C, 8 µl of a mix (see table below) containing reverse transcriptase buffer, a nucleotide mix and RNAse inhibitor were added per 12 µl sample. In the negative controls, 1 µl of H_2O (aqua a.i.) were included in the mix, while 1 µl RevertAid M-Mul V Reverse Transcriptase enzyme was added in the cases were the samples should be transcribed. (see table 13) The reverse transcription was performed at 42°C for one hour and terminated at 70° C for 10 minutes on heating blocks.

Table 13| Recipe: Mastermix for reverse transcription and polymerase chain reaction (RT-PCR)

Mix for reverse transcription and PCR (RT-PCR)	
4 µl	5x reaction buffer for M-Mul V RT
2 µl	PCR nucleotide mix 10 mM
1 µl	RiboLock RNAse Inhibitor
1 µl	RevertAid H Minus M-Mul V reverse transcriptase

PCR

The generated cDNA was used as template for a PCR with primers annealing within the genes encoding for GAPDH, RIG-I, TLR-2, -3, -4 and TLR-9. The PCR was performed using a PCR-mix containing aqua dest., Taq Polymerase Buffer and a nucleotide mix. In the case of GAPDH 2.5 µl cDNA template were added and 0.5 µl forward and 0.5 µl reverse primer were used. In the end 0.25 µl of Taq DNA Polymerase were added to start the reaction. (Table 14) For RIG-I, TLR-2, -3, -4 and TLR-9 1 µl DNA-template, 0.5 µl primermix (foreward and reverse sequence 1:1, see Table 15) and 0.5 µl Taq polymerase were added (see Table 16). The optimal thermocycler programs for the PCR were as follows:

For RIG-I, TLR-2, -3, -4 and TLR-9

95°C 5 minutes,

2x [95°C 30 sec; 62°30 sec; 72°C 30 sec]

2x [95°C 30 sec; 60°C 30 sec; 72°C 30 sec]

2x [95°C 30 sec; 58°C 30 sec; 72°C 30 sec]

30x [95°C 30 sec; 56°C 30 sec; 72°C 30 sec]

72° C 10 min

10° C store

For GAPDH

95°C 2 minutes,

30x [95°C 30 sec]

30x [55°C 30 sec]

30x [72°C 30 sec]

72° C 2 min

4° C store

Table 14| Recipe: Mastermix for polymerase chain reaction (PCR) for GAPDH

Mix for polymerase chain reaction (PCR) for GAPDH	
18.25 µl	Aqua a.i.
2.5 µl	PCR reaction buffer 10x conc.
0.5 µ	PCR nucleotide mix 10 mM

Table 15| Primers for polymerase chain reaction (PCR)

Primers	Forward sequence	Reverse sequence
GAPDH	5' –tga tga cat caa gaa ggt gtt gaa- 3'	5' –tcc ttg gag gcc atg tgg gcc at -3'
RIG-I	5' –ttg cta tcg ggt caa ca -3'	5' –caa aag agc atc cag caa ca -3'
TLR-2	5' –tga tgc tgc cat tct cat tc -3'	5' –cgc agc tct cag att tac cc -3'
TLR-3	5' –acc cat acc aac atc cct ga -3'	5' –gcc ctc aaa gtg gat gag aa -3'
TLR-4	5' –tga gca gtc gtg ctg gta tc -3'	5' -cag ggc ttt tct gag tcg tc -3'
TLR-9	5' –cta cga tgc ctt cgt ggt ct -3'	5' –gcc cac agg ttc tca aag ag -3'

Table 16| Recipe: Mastermix for polymerase chain reaction (PCR) for RIG and toll-like receptors (TLRs)

Mix for polymerase chain reaction (PCR) for RIG and toll-like receptors (TLRs)	
42.5 µl	Aqua a.i.
5 µl	PCR reaction buffer 10x
0.5 µl	PCR nucleotide mix 10 mM

10 µl of the PCR products were mixed with 5 µl DNA loading buffer each and fractionated on a 1% agarose gel containing ethidium bromide (see table 17). Electrophoresis was run at 125 V for 15-30 minutes. DNA bands were visualized with UV-light and analyzed using GelDoc software. As a marker 10 µl of New England Biolabs 100 bp ladder were run.

Table 17| Recipe: Gelelectrophoresis agarose gel

Gelelectrophoresis agarose gel	
1% agarose gel containing	1% (10 mg/ ml) Agarose
2.5 µg	Ethidiumbromid solution

2.2.7 Fluorescence in situ hybridization (FISH)

Solutions

Table 18| Recipe: Methanol:Acetic acid 3:1

Methanol: Acetic acid 3:1	
75 ml	Methanol p.A.
25 ml	Acetic acid 100% anhydrous

Table 19| Recipe: Pepsin solution

Pepsin solution	
1 mg	Pepsin from gastric porcine mucosa lyophilized powder
In 20 ml	water

Table 20| Recipe: 0.5 M $MgCl_2$

0.5 M $MgCl_2$	
16,6 g	$MgCl_2$ 3M
83.3 ml	H_2O

Table 21| Recipe: Phosphate Buffered Saline (PBS)/ $MgCl_2$

Phosphate Buffered Saline (PBS)/ $MgCl_2$	
40 ml	0.5 M $MgCl_2$ (see Table 20)
360 ml	1 x PBS

Table 22| Recipe: 1% formaldehyde solution

1% formaldehyde solution	
68 ml	Phosphate Buffered Saline (PBS)/ $MgCl_2$ (see Table 21)
2 ml	37% formaldehyde solution

Table 23| Recipe: Deionized formamide

Deionized formamide	
1L	Formamide
50 g	Mixed bed resin

Table 24| Recipe: 0.05 M NaH_2PO_4 x 2 H_2O- Buffer

0.05 M NaH_2PO_4 x 2 H_2O- Buffer	
3,9 g	NaH_2PO_4
500 ml	H_2O
11 ml	1 M NaOH

Table 25| Recipe: Fluorescence in situ hybridization (FISH) Denaturation mix

Denaturation mix	
49 ml	Deionized formamide (see Table 23)
7 ml	20 x saline-sodiumcitrate (SSC)
7 ml	0.05 M NaH_2PO_4 x 2 H_2O- Buffer (see Table 24)
3 drops from a 3 ml pasteur pipette	25% HCl
Filled up to 70 ml with	H_2O

Table 26| Recipe: Fluorescence in situ hybridization (FISH) Wash A

Wash A	
150 ml	formamide
30 ml	20x saline-sodiumcitrate (SSC)
3 drops from a pasteur pipette	25% HCl
filled up to 300 ml with	Aqua dest.

Table 27| Recipe: Fluorescence in situ hybridization (FISH) Wash B

Wash B	
2.5 ml	20x saline-sodiumcitrate (SSC)
Filled up to 500 ml with	H_2O

Table 28| Recipe: DAPI solution

DAPI solution	
14 µl	DAPI 1000 ng/ml
70 ml	20x SSC

<u>FISH protocol</u>

Chromosomal regions or specific genes of interest can be visualized by hybridization of a fluorescently labelled probe to the complementary DNA strand.

In our procedure 1.6 x 10^5 cells (i.e. MΦ, PBMCs) were harvested from culture dish. They were resuspended in 160 µl PBS. Cytospots were prepared by centrifugation at 800 rpm for 4 minutes. In this way, the cells were transferred onto an object slide and were fixed immediately in methanol:acetic acid 3:1 (see Table 18) for 5 minutes at room temperature. The slide then was placed in an appropriate pre-warmed jar containing 100 ml of 10 mM HCl with freshly added 200 µl of a 50 ng/ml pepsin solution (see Table 19). The slide was kept in the jar at 37°C in a water bath for 3 to 15 minutes, depending on the morphology of the examined cell type. Subsequently cells were washed in 2 x SSC for 5 minutes at room temperature. Fixation of the nuclei was performed in 1% formaldehyde

solution (see Table 22) for 15 minutes. Then, slides were air-dried and denaturation of double-DNA strands was initiated: the slides were incubated in a pre-warmed denaturation mix containing deionized formamide (see Table 25) at 75°C for exactly 2 minutes. After serial dehydration in 70%, 90% and 100% ethanol for 5 minutes on ice, the samples were air-dried. 2-10 µl probe were applied to the nuclei. If necessary, prior denaturation was performed according to the respective manufacturer recommendations. Cover glasses were attached to the slides and hybridization took place in a slightly wet box in the dark at 37°C overnight. From now on, the samples were kept in the dark. Cover glasses were removed and the cells were washed three times for 5 minutes at 42°C in Wash A containing formamide (see Table 26). A second washing step in diluted SSC (Wash B, see Table 27) was performed the same way at 60°C.
Cell nuclei were counterstained in a DAPI solution (see Table 28) for 30 seconds at room temperature.
Vecta shield mounting medium and cover glasses were applied to the slides before analysis of the gene labelling at the fluorescence microscope.

3. Results

3.1 HCMV infection rates are higher in M2-MΦ than in M1-MΦ

M1-MΦ and M2-MΦ, harvested after 7 days of monocyte stimulation with either GM- or M-CSF growth factors, were infected with moi 5 and 0.5 of the highly endotheliotropic HCMV strain TB40E. At 16-18 hours post infection (pi), corresponding to an overnight incubation at 37°C, mock- and HCMV-infected MΦ were fixed, permeabilized and processed for the measurement of the expression of IE1-2 gene products (immunofluorescence staining described in the *Materials and Methods* section).

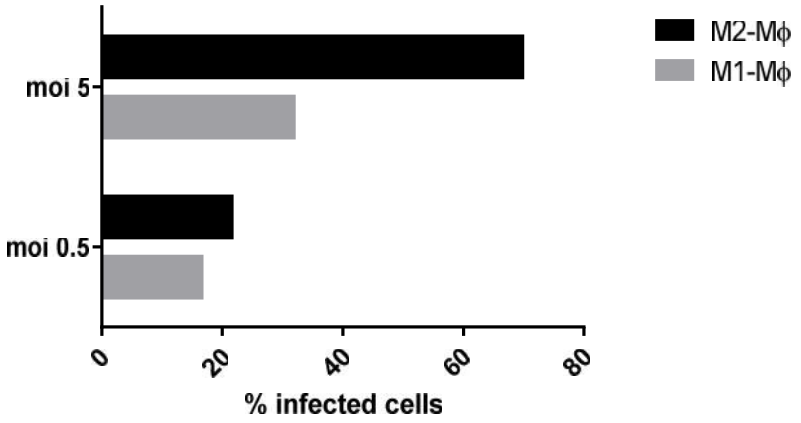

Figure 8: Infection rates of Human Cytomegalovirus (HCMV) in M1-Monocyte-Derived Macrophages (MΦ) and M2- MΦ. M1-MΦ and M2-MΦ were infected with Human Cytomegalovirus strain TB40E with either a multiplicity of infection (moi) of 0.5 or 5 and left in culture for one night at 37°C. Untreated, mock-infected samples were included as control. After fixation the infection rates were detected using an antibody raised against the viral protein IE1-2 and indirect immunofluorescence staining. The percentage of infected cells was calculated by counting the nuclei stained positively for IE1-2 per DAPI stained nuclei in five pictures taken at a magnification of 10x.

Counting of IE1-2 positive nuclei amongst nuclei stained by DAPI confirmed the earlier observations and as shown in Figure 8 at the multiplicity of infection (moi) of 0.5 an average of 21.5% of M2-MΦ were infected whereas in only 16.5% of M1-MΦ the virus replication cycle was initiated. At the moi 5 the infection rates were

69.7% and 31.8% in M2-MΦ and M1-MΦ, respectively. As expected, mock-infected MΦ did not express IE1-2 proteins. (Figure 8) Because these results confirmed already published [8] data the experiment was only carried out once.

3.2 Expression of putative HCMV receptors on M1-MΦ and M2-MΦ

Until now various cellular receptors have been suggested as entry receptors for HCMV into MΦ. In order to test the hypothesis that the higher susceptibility to HCMV infection exhibited by M2-MΦ depends on a faster and more abundant viral entry than in M1-MΦ, the expression of these molecules were compared in M1- and M2-MΦ.

3.2.1 CD13

3.2.1.1 CD13 surface expression is similar on M1- and M2-MΦ

Measurement of CD13 surface expression was performed by FACS applying the monoclonal antibody anti-CD13 clone WM15 at a concentration of 50 ng/ml. Isotypic control was the mouse antibody IgG1κ diluted 1:3 in order to reach the same concentration as the specific antibody.

As can be seen in one representative example (Figure 9), both M1- and M2-MΦ, were highly positive for the expression of CD13 on their surface. With an average percentage of approximately 100% in both cell types, the number of cells expressing CD13 on their surface was almost identical in the two subsets. The levels of expression on the single cell, represented by the mean intensity of fluorescence (MFI) values, were similar as well on the two cell types.

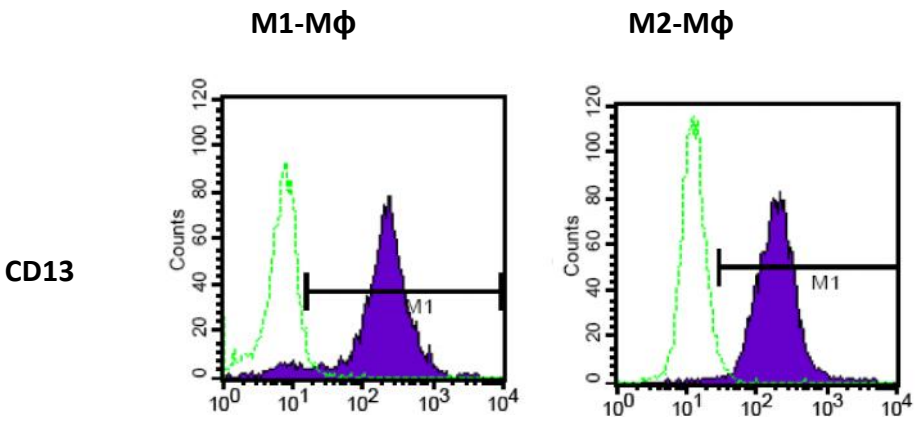

Figure 9: Fluorescence activated cell sorting (FACS) analysis of CD13 expression on the surface of M1-Monocyte-Derived Macrophages (MΦ) and M2- MΦ. Cells were incubated with either anti-CD13 antibody or isotypic control for one hour in the dark at 4°C. The purple area represents the signal given by the antibody anti-CD13, while the green dashed histograms represent the signal given by the isotypic control. The signal included in the marked region M1 was considered as specific because of the higher rate than the signal for the isotype control IgG1κ. Histograms are representative of one out of three blood donors.

A comparative analysis performed on cells obtained from three different blood donors (Figure 10) revealed that no significant differences could be found for the values of positively stained cells nor for mean fluorescence intensities.

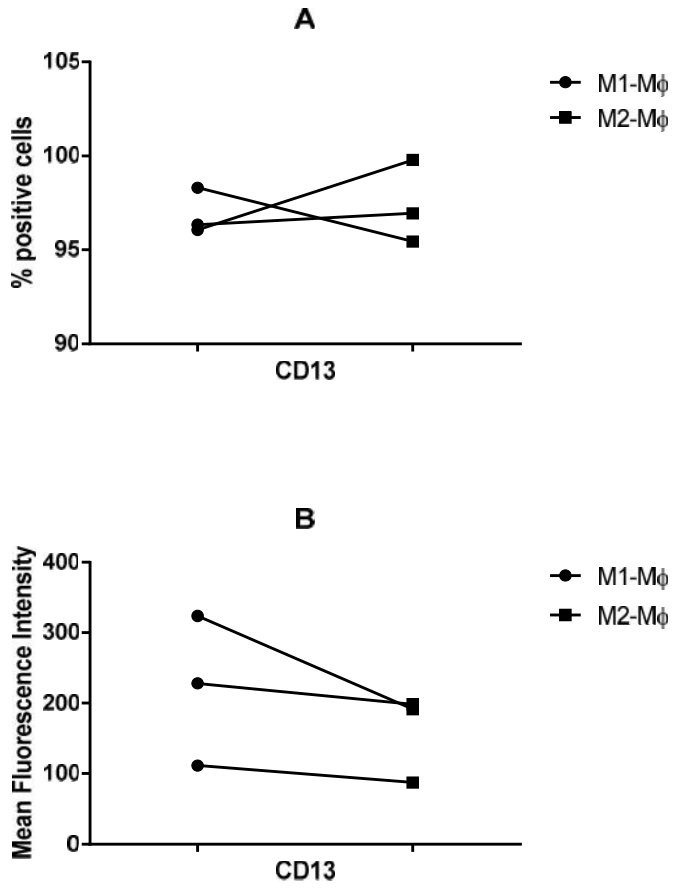

Figure 10: Expression of CD13 in M1-Monocyte-Derived-Macrophages (MΦ) and M2- MΦ. Expression of CD13 in M1- and M2-MΦ was evaluated in three different donors using anti-CD13 antibody by fluorescence cytometry. This shows total percentage of cells expressing the surface molecule (A) and the mean intensity of fluorescence per cell (B) as measured by Fluorescence activated cell sorting (FACS).

3.2.1.2 Blocking of CD13 by specific antibodies in M1- or M2-MΦ did not lead to reduced infectivity rates

In order to estimate the significance of CD13 in the process of HCMV entry into MΦ blocking of CD13 was performed by incubating about 1,2 x 10^5 cells with 500 ng/ml of either anti-CD13 or the immunoglobulin concentrate Gammunex®. The latter can completely impair HCMV infectivity in MΦ.

Cells were incubated for half an hour at 37°C with the anti-CD13 antibodies and Gammunex®. During this time attachment to the cellular antigens was assumed to have happened.

Afterwards cells were infected with the HCMV laboratory strain TB40E at a moi of 5. After three hours at 37°C medium was changed in order to avoid delayed/asynchronous HCMV

infection. 21 hours later cells were fixed, permeabilized and stained with anti-IE1-2 antibody in order to quantify the infection rates.

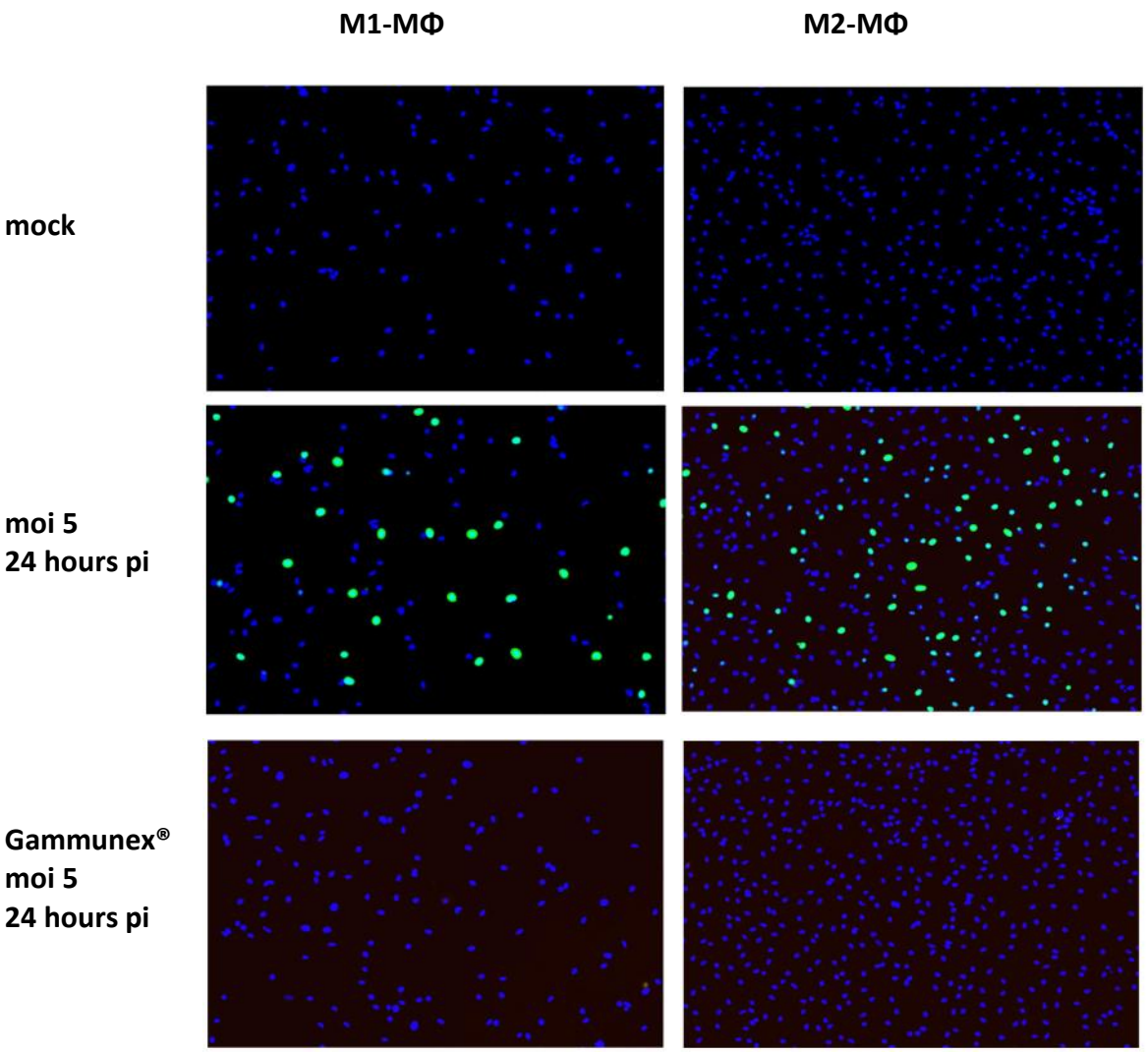

Figure 11: Human cytomegalovirus (HCMV) infection of M1- and M2-Monocyte-Derived Macrophages (MΦ) is inhibited by immunoglobulin concentrate Gammunex® 1.2 x 10^5 M1- and M2-MΦ were left untreated or incubated with immunoglobulin concentrate Gammunex®. 30 minutes later, M1- and M2-MΦ were mock- and HCMV-infected (TB40E; multiplicity of infection (moi) of 5). 3 hours later unabsorbed virus was removed and new medium was added for additional 21 hours. At 24 hours after infection, M1- and M2-MΦ were fixed and stained with anti-IE1-2 antibodies (green) and DAPI (blue). Pictures (magnification 10x) are from one experiment representative of three.

As shown in Figure 11 Gammunex® efficiently blocked HCMV infection when incubated on cells half an hour before virus infection, leading to infection rates as low as 0.4 (±

0.69) % in M1-MΦ and 0 (± 0) % in M2-MΦ as compared to 8.4 (± 10.74) % in M1-MΦ and 22.07 (± 5.95) % in M2-MΦ when infection was performed without immunoglobulins.

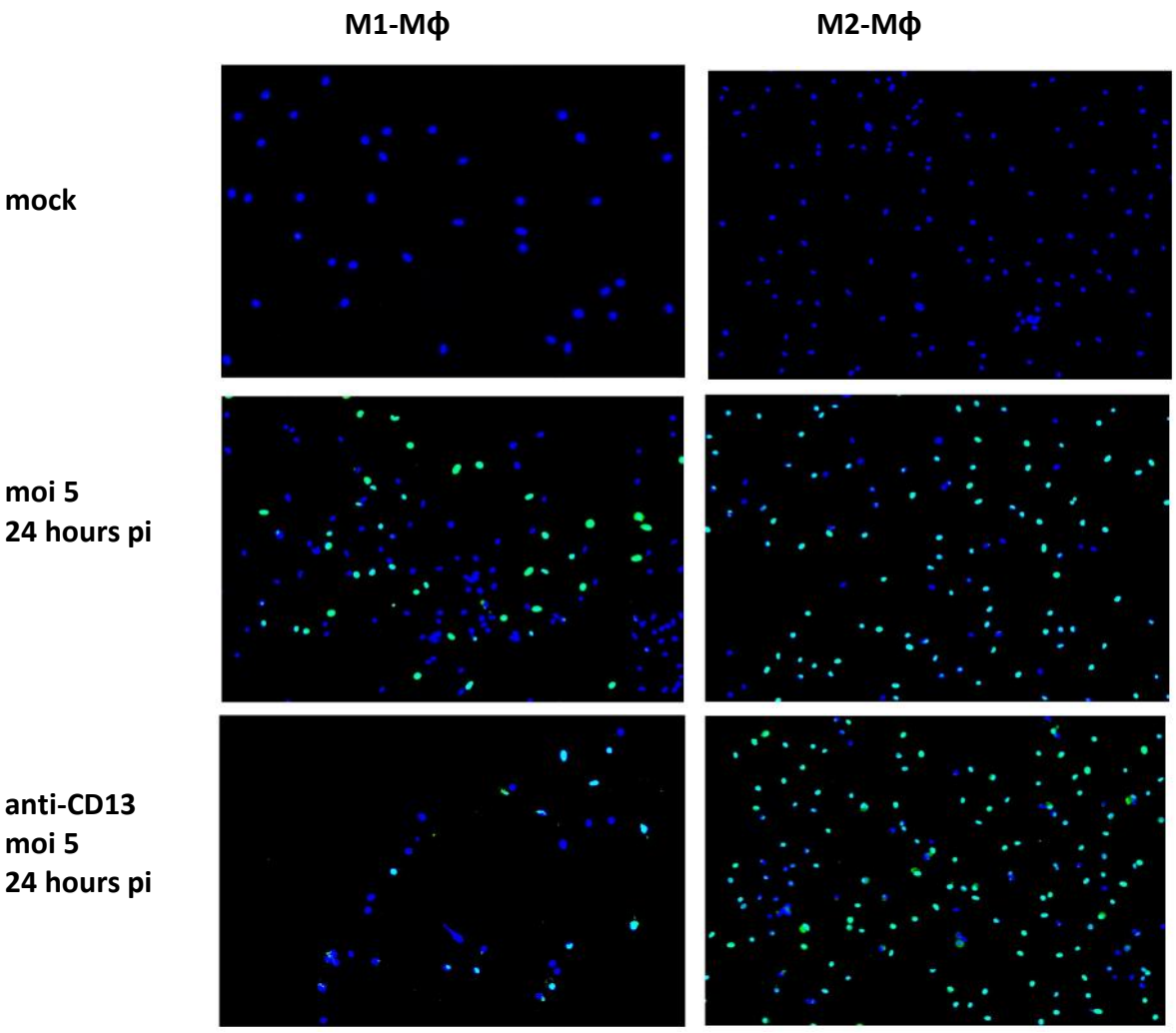

Figure 12: Human Cytomegalovirus (HCMV) infection of M1-Monocyte-Derived Macrophages (MΦ) and M2-MΦ is not inhibited by anti-CD13 antibodies. 1.2 x 10^5 M1- and M2-MΦ were left untreated or incubated with 500 ng/ml of anti-CD13 antibodies. 30 minutes later, M1- and M2-MΦ were mock- and HCMV-infected (TB40E; multiplicity of infection (moi) of 5). 3 hours later unabsorbed virus was removed and new medium was added for additional 21 hours. At 24 hours after infection, M1- and M2-MΦ were fixed and stained with anti-IE1-2 antibodies (green) and DAPI (blue). Pictures (magnification 10x) are from one experiment representative of three blocking experiments.

On the contrary, the cell treatment with anti-CD13 antibodies (Figure 12), did not lead to any significant reduction of infection and the viral cycle started in 16.37 (± 8.76) % of M1-

MΦ after pretreatment with the antibody as compared to 19.97 (± 13.91) % of M1-MΦ without treatment. The same was true for M2-MΦ and while cells exposed to anti-CD13 were infected as high as 45.17 (± 31.31) %, 47.57 (± 31.43) % of M2-MΦ were infected when cells were not treated. (see also Figure 13)

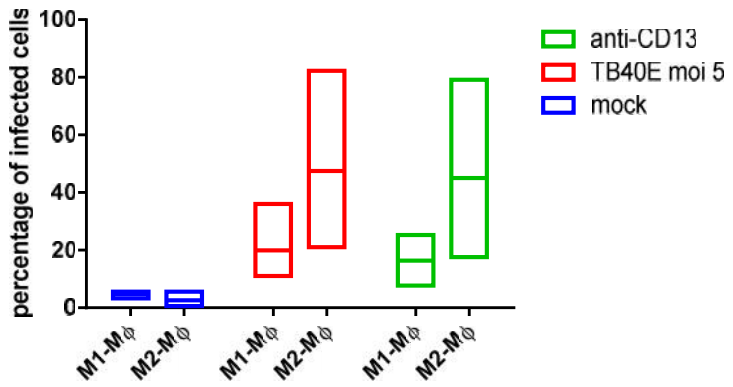

Figure 13: Human cytomegalovirus (HCMV) infectivity rates in M1-Monocyte-Derived Macrophages (MΦ) and M2-MΦ before and after blocking of CD13. Cells were left uninfected, infected with HCMV strain TB40E with a multiplicity of infection (moi) of 5 or incubated with specific antibody against CD13 for 30 minutes before infection. Indirect immunofluorescence staining for viral protein IE 1-2 was performed at 24 hours pi. Percentage of infected cells was detected by counting of DAPI positive nuclei stained for IE1-2 per picture taken by fluorescence microscopy at a magnification of 10x. Mean, minimum and maximum of Infectivity rates obtained from three independent experiments are shown as horizontal lines.

Although drawing conclusions concerning the blocking experiments has to be done somewhat carefully (see *Discussion*), one possible assumption is that CD13 might not be the major component enabling HCMV to enter M2-MΦ more efficiently than M1-MΦ.

3.2.2 Similar surface expression of integrin chains on M1- and M2-MΦ

In this study, the expression of different types of integrins was quantified on the surface of M1- and M2-MΦ by mean of FACS analysis.

0.6 x 10^6 cells of each of the two MΦ subtypes were detached from culture dishes and processed for FACS staining using various fluorescent antibodies specific for different integrin chains at the concentrations specified by the manufacturer instructions.

The examined integrin chains were (in the order of their clusters of differentiation) alpha-L, alpha-X, alpha-M, beta-2, beta-1, alpha-2b, alpha-4 and beta-3.
As can be seen in one representative example (Figure 14), the integrin expression profiles were comparable in M1-MΦ and M2-MΦ and no clear differences could be seen. Taking into account the corresponding isotypic controls, all examined integrin chains were found to be clearly expressed on the surface of both M1- and M2-MΦ, except alpha-2b and beta-3, which could not be detected on either cell type.
As depicted in Figure 15, alpha-L, alpha-M, alpha-X, beta-1 and beta-2 chains were expressed by the majority of MΦ at relatively high levels. Expression of alpha-2b, alpha-4 and beta-3 were very low or undetectable. Despite the great variability between values obtained from cells produced form different blood donors, a trend could be observed. The highly expressed alpha-L, alpha-M and beta-1 seemed to be expressed at relatively similar levels in M1- and M2-MΦ.
For alpha-X and beta-2 chains a slight difference could be detected. The MFI values of alpha-X were higher on M2-MΦ than M1-MΦ in all experiments. The total percentage of cells expressing alpha-X was either higher in M2-MΦ, too, or similar for both cell subtypes. MFI values of beta-2 appeared to be higher in M1-MΦ than M2-MΦ in all experiments.

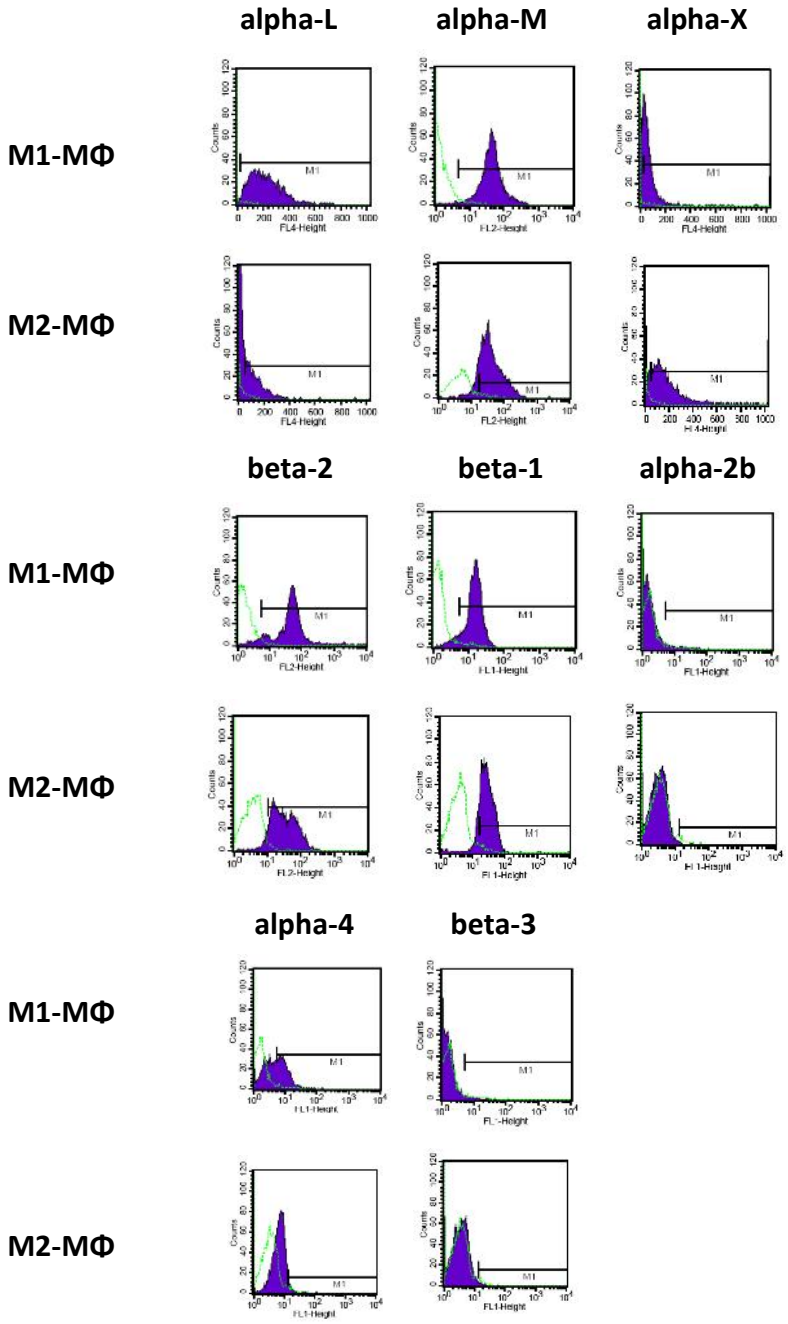

Figure 14: Analysis of integrin expression on the surface of M1-Monocyte-Derived-Macrophages (MΦ) and M2-MΦ. Cells were incubated with the indicated antibodies for one hour in the dark at 4°C. While the green dashed lines represent the adequate isotype control IgG1 (fluorescein isothiocyanate (FITC), phycoerythrin (PE) or allophycocyanin (APC)), the purple areas represent cells positive for the staining with the corresponding antibody. The percentage of positive cells was calculated within the borders of the so-named "M1"-marker. The histograms show representative data of one out of three experiments.

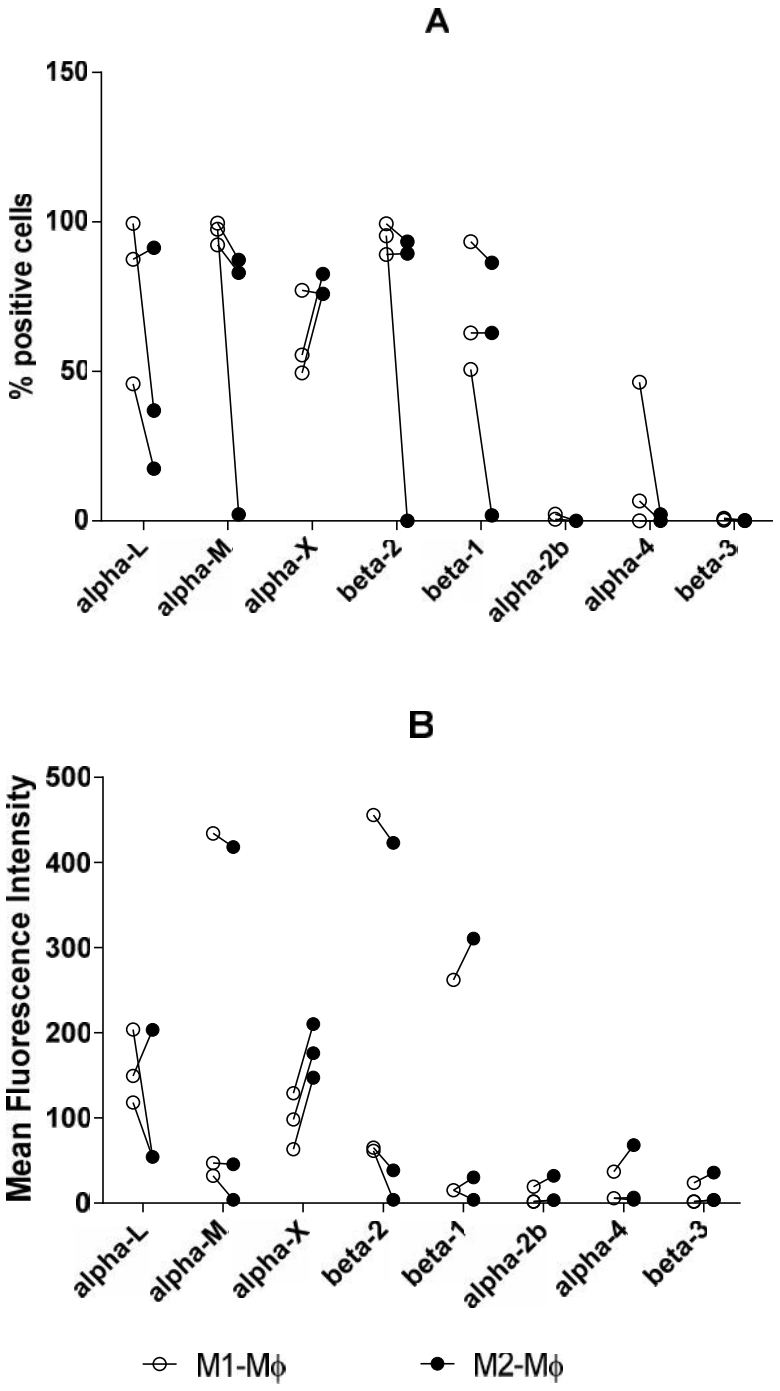

Figure 15: Analysis of integrin chain expression on M1-Monocyte-Derived Macrophages (MΦ) and M2-MΦ. Expression of integrins on the surface of M1- and M2-MΦ was evaluated in three different donors using specific antibodies recognizing the indicated chains. The percentages of positive cells (A) and the mean fluorescence intensity values (B) are shown for M1- (white dots) and M2- (black dots) MΦ. MΦ obtained from the same blood donor are connected by a line.

Due to the high interdonor variability it is not possible to draw conclusive statements and though interesting the two observations of a differential expression of alpha-X and beta-2 have to be confirmed by investigating additional cell preparation.

3.2.3 BST2/ Tetherin surface expression was higher on M2-MΦ than M1-MΦ in 4 of 5 experiments

Measurement of expression of tetherin on the surface of M1- and of M2-MΦ was performed by FACS analysis.

One million cells of each subtype were resuspended and incubated with the primary anti-BST2 mouse antibody diluted 1:200 as described in *Materials and Methods* and subsequently with a secondary anti-mouse PE antibody diluted 1:20 for 30 minutes at 4°C in the dark. As an isotypic control a sample with unstained cells was used because they showed a fluorescence signal similar to the one of IgG1κ, an isotypic control used in other experiments.

As can be seen in Figure 16 the expression of BST2 showed significant donor variability. However, within individual experiments, the percentage of cells expressing BST2 was higher in M2-MΦ than in M1-MΦ in all but one cell preparation where this phenomenon was inverted. The same was observed for the values of mean fluorescence intensity: levels were higher in M2-MΦ than M1-MΦ, except in the aforementioned single experiment. (see also representative example in Figure 17)

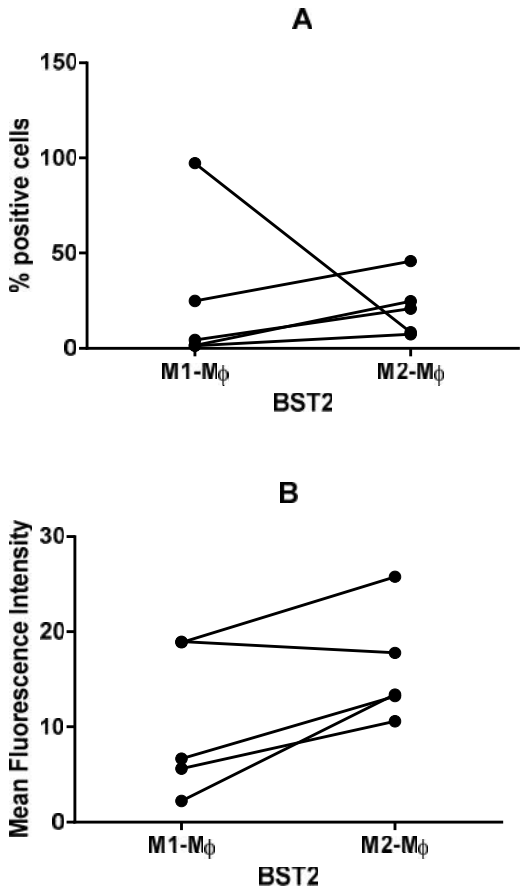

Figure 16: Bone marrow stromal antigen 2 (BST2) expression in M1- and M2- Monocyte-Derived macrophages (MΦ). BST2 expression in M1-and M2-MΦ was evaluated in five different donors using anti-BST2 antibody. The percentage of cells expressing the surface molecule (A) and the mean fluorescence intensity values of BST2 per cell (B) are shown.

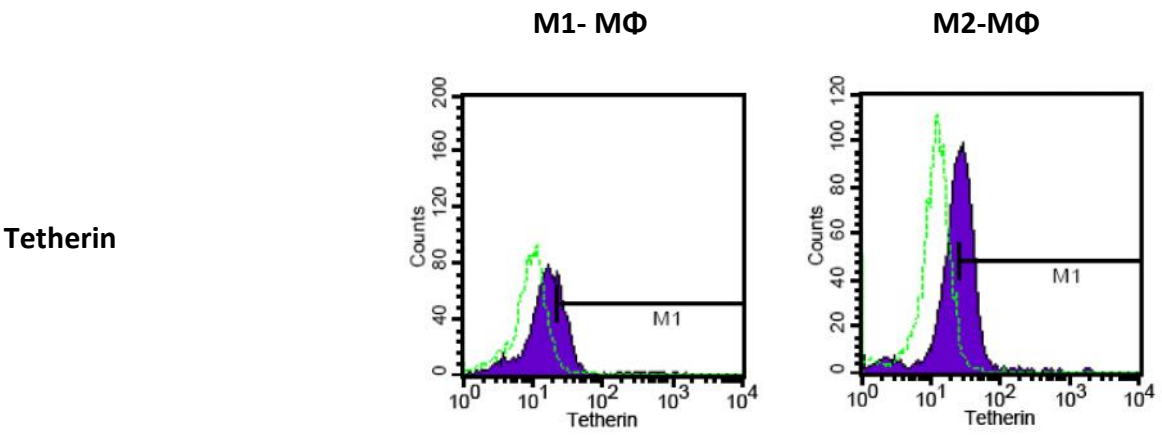

Figure 17: FACS analysis of Bone marrow stromal antigen 2 (BST2)-expression in M1- and M2- Monocyte-Derived macrophages (MΦ). Cells were incubated with anti-BST2 antibody for one hour in the dark at 4°C. While the green dashed lines represent the signal given by the secondary anti-mouse phycoerythrin (PE) antibody alone, the purple areas represent the signal given by the anti-BST2 antibody and the secondary anti-mouse PE. The percentage of positive cells was calculated within the borders of the so-named "M1"-marker.Histograms are obtained from one representative cell preparation out of five.

Although preliminary these data indicate that BST2 might have a role as an entry receptor to HCMV since M2-MΦ, the subset more susceptible to infection, seem to express higher levels of this protein.

3.2.4 EGFR is not expressed in M1- and M2-MΦ

In order to investigate the role of EGFR during HCMV infection of MΦ, the expression of this receptor on cells was quantified by flow cytometry analysis.
While the monocyte and macrophage population marker CD14 was used as positive control, the immunoglobulins IgG2b served as isotypic controls. One million cells were resuspended as decribed in *Materials and Methods* and the same concentration of anti-EGFR and IgG2b immunoglobulins were added.

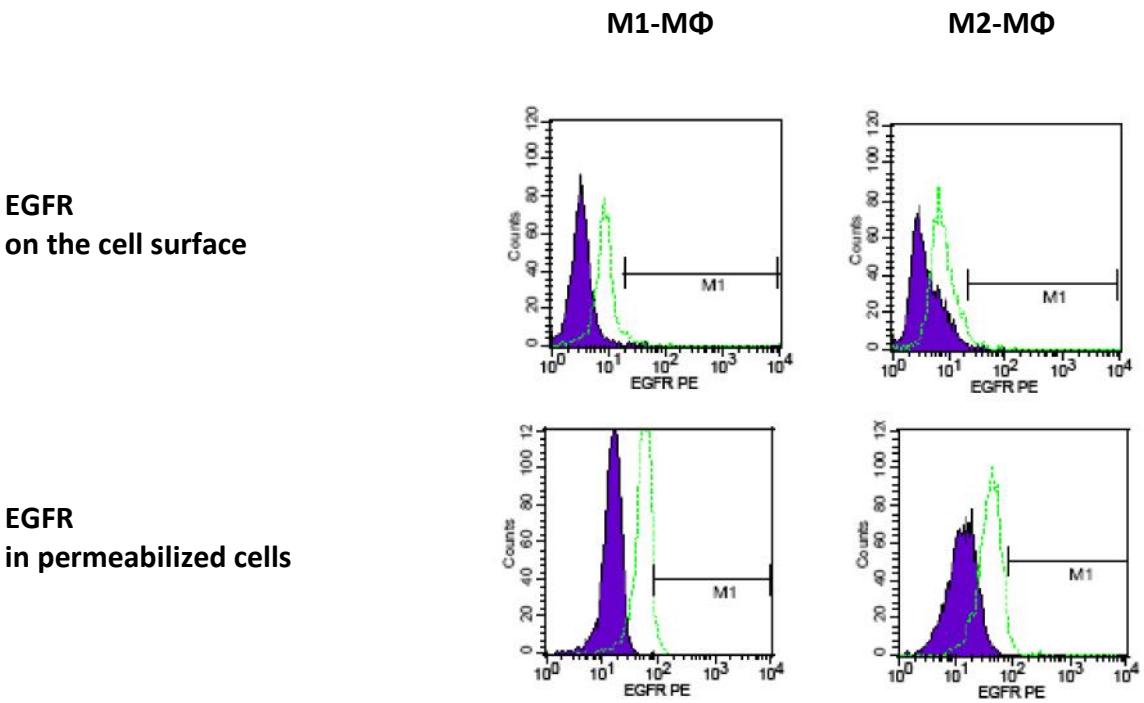

Figure 18: Expression of epidermal growth factor receptor (EGFR) on the surface and after permeabilization of M1- and M2-Monocyte-Derived Macrophages (MΦ). For the surface staining, cells were incubated with anti-EGFR antibody (EGFR phycoerythrin (PE)) for one hour in the dark at 4°C before quick fixation and analysis at the cytofluorimeter. For the total staining, cells were fixed and permeabilized with Cytofix/Cytoperm kit according to manufacturer instruction and then incubated with anti-EGFR antibody (EGFR PE) for one hour in the dark at 4°C before. The purple area represents the signal resulting from the anti-EGFR antibody, while the green dashed lines represent the isotype control IgG2b. The percentage of positive cells was calculated within the borders of the so-named "M1"-marker. Representative data from one of three experiments are shown.

In all experiments, the surface expression of EGFR was not detectable on M1- nor M2-MΦ. Mean fluorescence intensity values were even lower than those of the isotypic control thus indicating a complete lack of detection.

On the contrary, the positive control surface receptor CD14 was detected clearly in M1- and M2-MΦ.

Since EGFR has been described as the most important receptor of HCMV and no signal could be detected herein in cells highly susceptible to infection, the possibility was considered that the receptor might not be exposed on the cell surface but remains in an

internalized state in MΦ. As shown in Figure 18, the expression of EGFR was investigated on non-permeabilized as well as permeabilized MΦ.
Results, however, were not different from investigations on surface expression. EGFR was not detected on the surface of or inside M1- or M2-MΦ, thus indicating that MΦ do not express EGFR on their surface or carry it within their cytoplasm.

3.2.5 PDGFR-α is not expressed in M1-MΦ and M2-MΦ

Like for EGFR, expression of PDGFR-α was examined in viable (cell surface) as well as in fixed/permebilized (intracellular staining) MΦ.
As described before, the monocyte and macrophage population marker CD14 was used as positive control and the immunoglobulin IgG2b served as isotypic controls. One million cells were resuspended and incubated with the same amount of anti-PDGFR-α and IgG2b immunoglobulins.
Similarly to EGFR, the PDGF receptor was not found on the surface of M1-MΦ or M2-MΦ (Figure 19) and the signal given by the specific antibody was equal or even lower than the signal given by the isotypic control.
This was also true for cells after permeabilization, as expression levels as measured by FACS were not increased.
On the contrary, positive control CD14 was nicely detected on M1- and M2-MΦ.

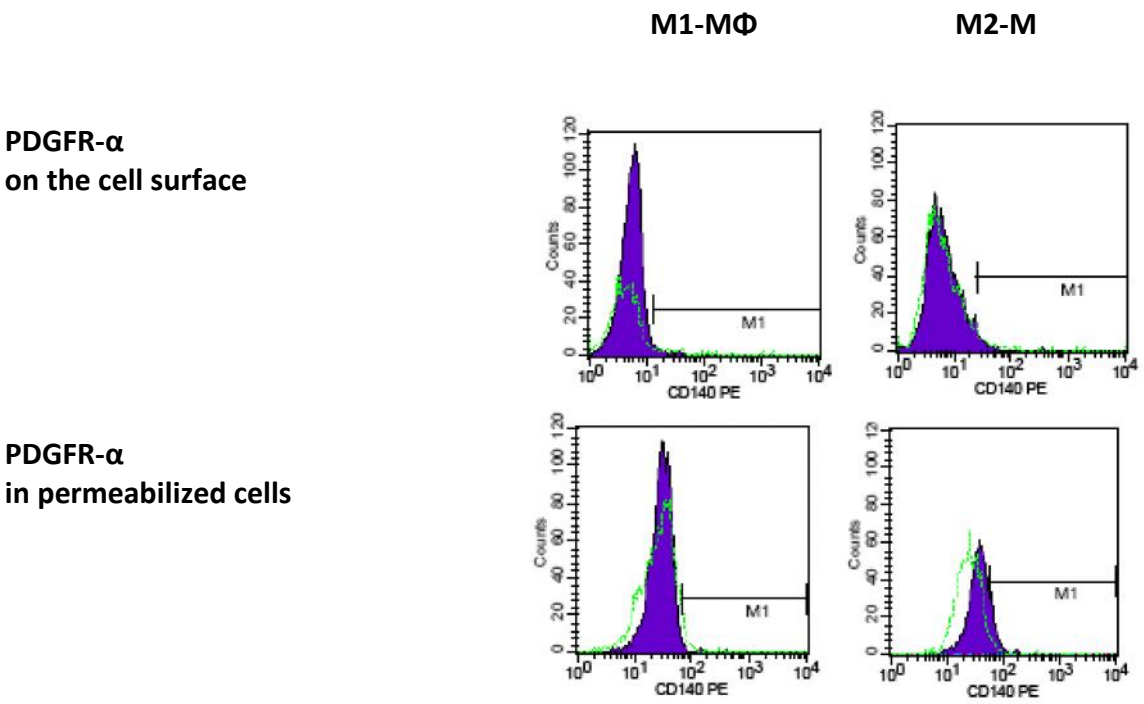

Figure 19: Expression of Platelet Derived Growth Factor α (PDGFR-α) on the surface and after permeabilizatin of M1- and M2-Monocyte-derived-Macrophages (MΦ). For the surface staining, viable cells were incubated with anti-PDGFR-α antibody (CD140 phycoerythrin (PE)) for 1 hour in the dark at 4°C before quick fixation and analysis at the cytofluorimeter. For the total staining, cells were fixed and permeabilized with Cytofix/Cytoperm kit according to manufacturer instruction and then incubated with anti-PDGFR-α antibody (CD140 PE) for 1 hour in the dark at 4°C before. The purple area represents the signal resulting from the anti-PDGFR-α antibody antibody, while the green dashed lines represent the isotype control IgG2b. The percentage of positive cells was calculated within the borders of the so-named "M1"-marker. Representative data from one of three experiments per setting are shown.

3.3 Translocation of HCMV proteins gB, pp65 and pp150 from the cell membrane to the nucleus takes place at a faster pace in M2-MΦ than in M1-MΦ

Approaching the question whether the difference in susceptibility to HCMV in M1- and M2-MΦ was already apparent at stages prior to viral DNA-replication, the intracellular movements of the viral particles were investigated in the two types of MΦ using indirect immunofluorescence assays. Thereby the structural virus proteins gB, pp65 and pp150 and their respective cellular localization were made visible at different time points after infection for fluorescent confocal microscopy.

M1-MΦ and M2-MΦ were infected with a moi 5 of the HCMV-strain TB40E. At 3 and 6 hours pi cells were fixed using 4% PFA and permeabilized with PBS 0.2% Triton-X-100 prior immunofluorescence staining using specific monoclonal antibodies against gB, pp65 and pp150.

As Figures 20-22 show, M1-MΦ as well as M2-MΦ showed a clear signal for gB, pp65 and pp150 suggesting that abundant viral particles entered in contact with both cell types. However, the intracellular distribution of the proteins did not look comparable in the two types of MΦ. Over a time course of 6 hours signals of all three molecules migrated faster and more efficiently towards the nucleus in M2-MΦ than in M1-MΦ.

As shown in Figure 20, the main envelope glycocoprotein gB seemed to move in direction of the cellular nucleus faster and more abundantly in M2-MΦ than in M1-MΦ.

3 hours pi the signal indicating viral gB was still in the periphery of M1-MΦ while in M2-MΦ it was already distributed over the entire cytoplasm. 6 hours pi the diffuse cytoplasmatic localization could also be observed in M1-MΦ, but meanwhile in M2-MΦ gB was predominantly found in very close proximity to the nucleus. In agreement with the expected localization of an envelope glycoprotein during infection, staining for gB was not detected within nuclei. Additionally, mock-infected cells did not show staining for gB at any time.

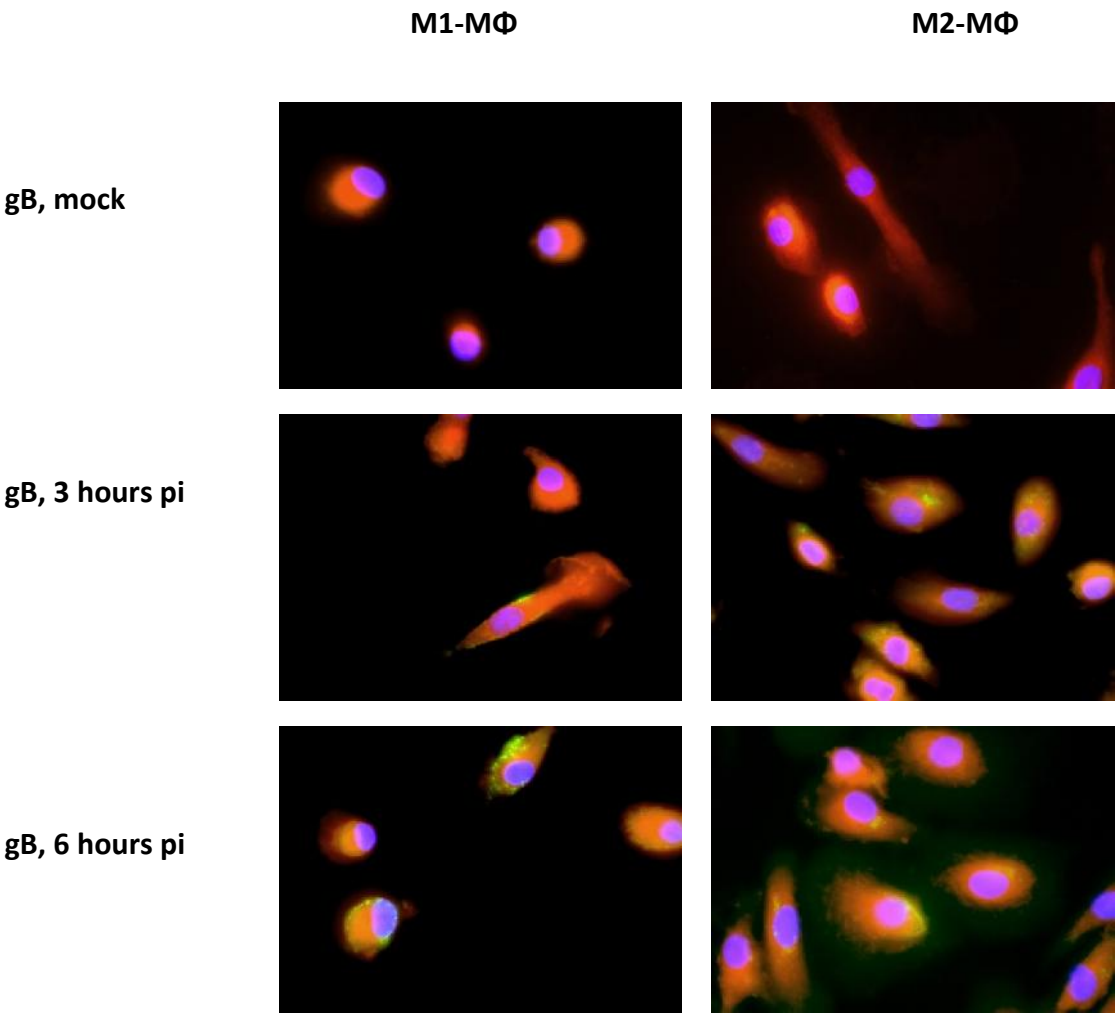

Figure 20: Kinetic analysis of glycoprotein gB (green) distribution in M1-Monocyte-Derived macrophages (MΦ) and M2-MΦ after Human cytomegalovirus (HCMV) infection. Cells were infected with TB40E (multiplicity of infection (moi) = 5) for 3 and 6 hours. After fixation cells were incubated with a specific antibody raised against glycoprotein gB and indirect immunofluorescence staining was carried out as described in *Materials and Methods*. gB is labelled in green, while nuclei and cytoplasm are counterstained with DAPI (blue) and Evansblue (red), respectively. Pictures (magnification 63x) are representative of three independent experiments.

As shown in Figure 21, the tegument protein pp65 was detected in the nuclei of roughly half of the M2-MΦ starting from 3 hours pi and the number of positive nuclei increased until 6 hours pi. In contrast, at 3 hours pi none of the M1-MΦ nuclei were positive and abundant pp65 signal localized perinuclearly. Only at 6 hours pi a small number of pp65

positive nuclei could be detected in the M1-MΦ sample but the majority of cells still presented a cytoplasmatic diffuse distribution.

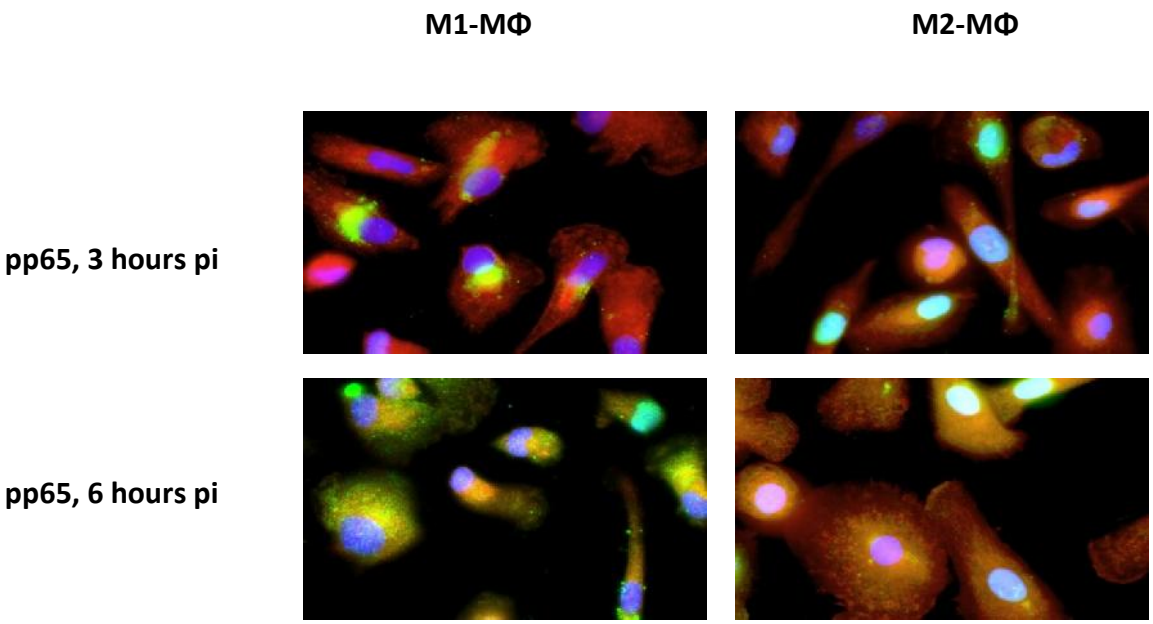

Figure 21: Kinetic analysis of pp65 (green) distribution in M1-Monocyte-Derived-Macrophages (MΦ) and M2-MΦ after Human Cytomegalovirus (HCMV) infection. Cells were infected with TB40E with a multiplicity of infection (moi) of 5 for 3 and 6 hours. After fixation cells were incubated with a specific antibody raised against the viral tegument protein pp65 (green), counterstained with DAPI (blue) and Evansblue (red) as described in Figure 20. Pictures (magnification 63x) are representative of three independent experiments.

As can be seen in Figure 21, the distribution pattern of pp150 was comparable to that of pp65, though the translocation towards the nucleus in general seemed to happen more slowly. At 3 hours pi in both M1-MΦ and M2-MΦ pp150 bordered the cell membrane and accumulated in vesicular aggregates that distributed throughout the cytoplasm and in proximity to the nucleus. In contrast, while at 6 hours pi pp150 could be detected in the nuclei of the majority of M2-MΦ, in M1-MΦ only few nuclei showed specific fluorescence for pp150 and the majority of cells exhibited a similar distribution pattern to the one observed at 3 hours pi.

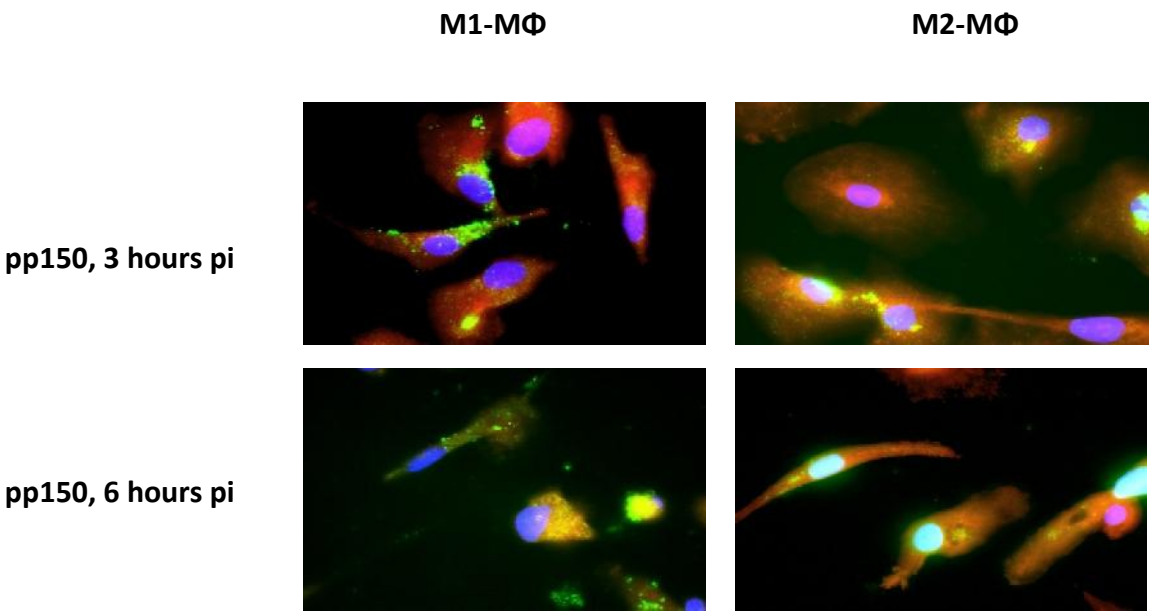

Figure 22: Kinetic analysis of pp150 (green) distribution in M1-Monocyte-Derived Macrophages (MΦ) and M2-MΦ after Human cytomegalovirus (HCMV) infection. Cells were infected with TB40E with a multiplicity of infection (moi) of 5 for 3 and 6 hours. After fixation cells were incubated with a specific antibody raised against the viral tegument protein pp150 (green), counterstained with DAPI (blue) and Evansblue (red) as described in Figure 20. Pictures (magnification 63x) are representative of three independent experiments.

In summary the data demonstrate a faster and more efficient migration of structural components of HCMV viral particles to the nucleus of M2-MΦ than M1-MΦ. Regarding the higher susceptibility to HCMV infection exhibited by M2-MΦ as compared to M1-MΦ a possible explanation could be that this phenomenon already origins from a difference in viral entry (see Chapter 3.2) and/ or viral translocation rather than for example dissimilar DNA-transcription or replication rates in the nucleus alone.

3.4 Performance of FISH was not successful in MΦ, but a protocol for FISH in PBMC could be established

Fluorescence in situ hybridization (FISH) allows the detection of specific DNA sequences within cellular nuclei. In this study, it represented a potential way to visualize the viral DNA delivered into the nucleus of a target host cell.

At first, a protocol for FISH was established in PBMC by applying a common positive control in cytogenetic procedures, namely the probe hybridizing to the cellular gene C-MET.

C-MET is located to chromosome 7 (7q31) and has a length of 420 kbp. Since C-MET can be present in a replicated form in cancer cells, more than two copies might be feasible in one cell. The probe used in these experiments was bought as ready-to-use and was applied following the manufacturer instructions after a denaturation at 90°C for 10 minutes. The chosen probe for C-MET is directly labelled with red Platinum*Bright*550 (red fluorescence) and is provided in combination with a probe for the centromer region of chromosome 7 fluorescently marked by greenPlatinum*Bright*495 (green fluorescence).

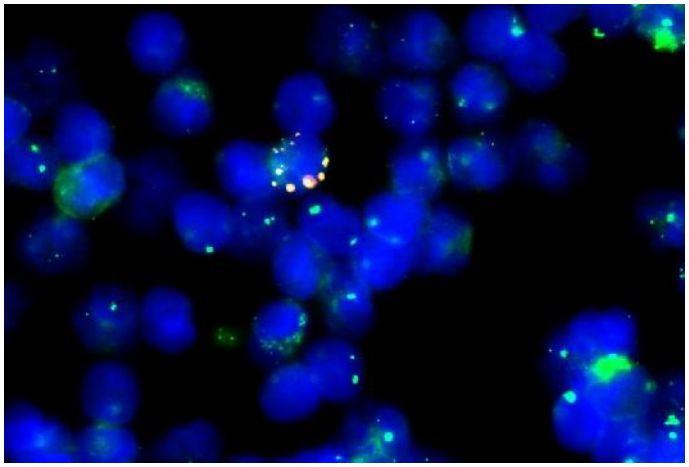

Figure 23: Fluorescence in situ detection (FISH) of cellular gene C-MET (red) and the centromeric region on chromosome 7 (green) in the nuclei of peripheral blood mononuclear cells (PBMC). PBMC were cytospotted, fixed and cellular peptides were digested by 5 minute incubation in a pepsin solution (0.1 ng/ml). DNA strands were denaturated with formamide at 75°C and dehydrated prior incubation with the specific probes. Hybridization with the C-MET probe was performed at 37°C overnight in the dark. Nuclei were counterstained with DAPI. The picture (magnification 100x) is representative of one experiment.

1.6 x 10^6 PBMC isolated from buffy-coat were transferred to object slides by centrifugation and FISH was performed as described in *Materials and Methods*.
As shown in Figure 23, centromers could be labelled by FISH and appeared as one or two green dots in the majority of the PBMC nuclei. Moreover, at least in some nuclei the staining for C-MET could also be visualized as minimum two red dots.
Plans were to broaden this technique to MΦ and, in a next step, to perform FISH in HCMV-infected cells using a probe specific for hybridization to viral genes and to quantify the genomes incorporated into the cell nuclei this way.
Unfortunately all attempts to detect C-MET in MΦ by FISH were not successful, supposedly because of different cell morphology, especially concerning cell size and resistance to pepsin digestion, and this technical approach had to be abandoned.

3.5 Analysis of putative intrinsic restriction factors for HCMV infection

Another possible explanation for the differing susceptibility of M1- and M2-MΦ to HCMV infection is that pathogen recognition receptors usually responsible for virus sensing are expressed in higher amount in M1- than in M2-MΦ and are then acting as intrinsic restriction factors.

3.5.1 TLRs -2, -3, -4 and RIG-I are expressed in M1-MΦ and M2-MΦ, TLR-9 might not be expressed in either cell type

Toll-like receptors and RIG-I have been previously described as factors playing a role in cell entry of HCMV [13,20,84]. In this project, due to the lack of reliable antibodies for FACS analysis, their expression in M1- as compared to M2-MΦ was evaluated by measuring transcription by RT-PCR.
1 x 10^6 cells of each subtype were detached from culture dish, their total RNA extracted and reversely transcribed into cDNA prior PCR analysis using a couple of primers designed for the housekeeping gene GAPDH.
As shown in Figure 24, the cDNA obtained from both M1- and M2-MΦ was of sufficient quality to allow the synthesis of the expected PCR product (250 bp size) corresponding to

the GAPDH amplificates. Since samples where the reverse transcriptase was not added did not allow the production of the PCR products it was concluded that the cDNA samples were free from contaminating genomic DNA.

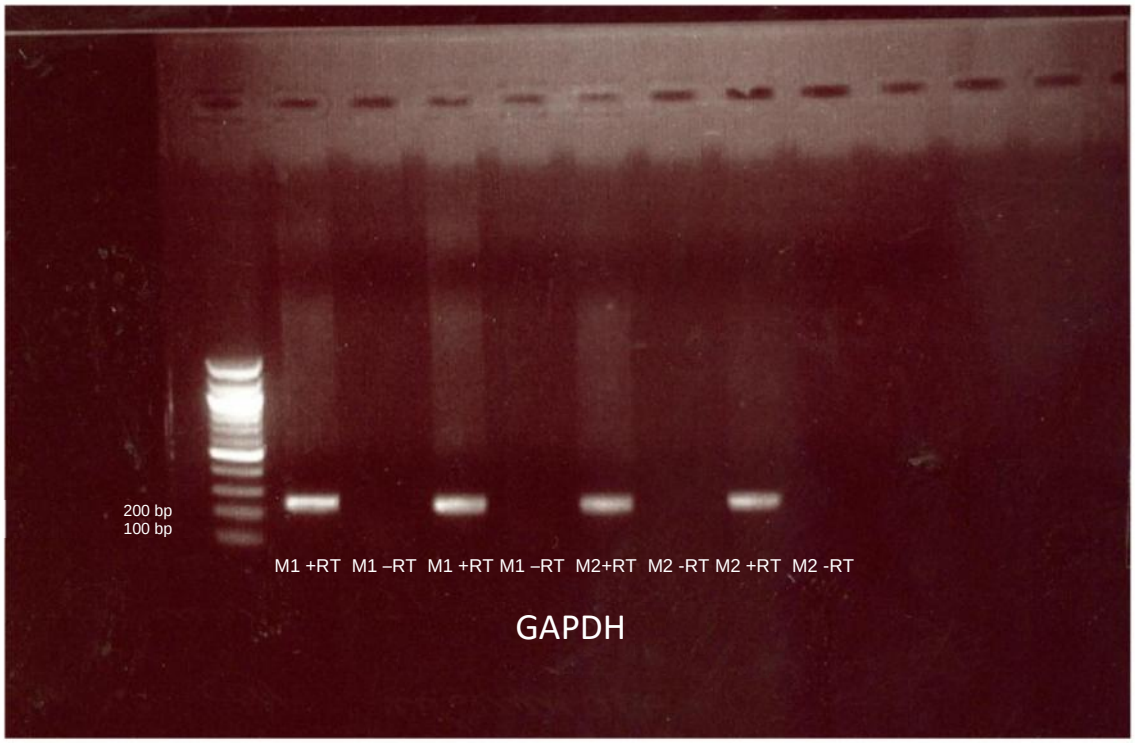

Figure 24: Expression of housekeeping gene GAPDH in M1-Monocyte-Derived Macrophages (MΦ) and M2-MΦ. RNA was isolated from M1- and M2-MΦ. Total RNA was either retro-transcribed into cDNA (indicated as +RT) or incubated without reverse transcriptase (indicated as –RT). The products of these reactions were used as templates for the polymerase chain reaction (PCR) with a couple of primers complementary to the GAPDH housekeeping gene. DNA ladder is run on the left; expected size of the PCR product is 250 base pairs (bp). Templates from the same donor were run twice for M1- and M2-MΦ each.

A similar approach was used to investigate the expression of RIG-I, TLR-2, -3, -4 and -9. As shown in Figure 25 no PCR products corresponding to RIG-I, TLR-2, -3, -4 and -9 could be found in the used negative control, distilled water. On the contrary, specific products for RIG-I, TLR-2, TLR-3 and TLR-4 could be found at similar intensities in both M1- and M2-MΦ.

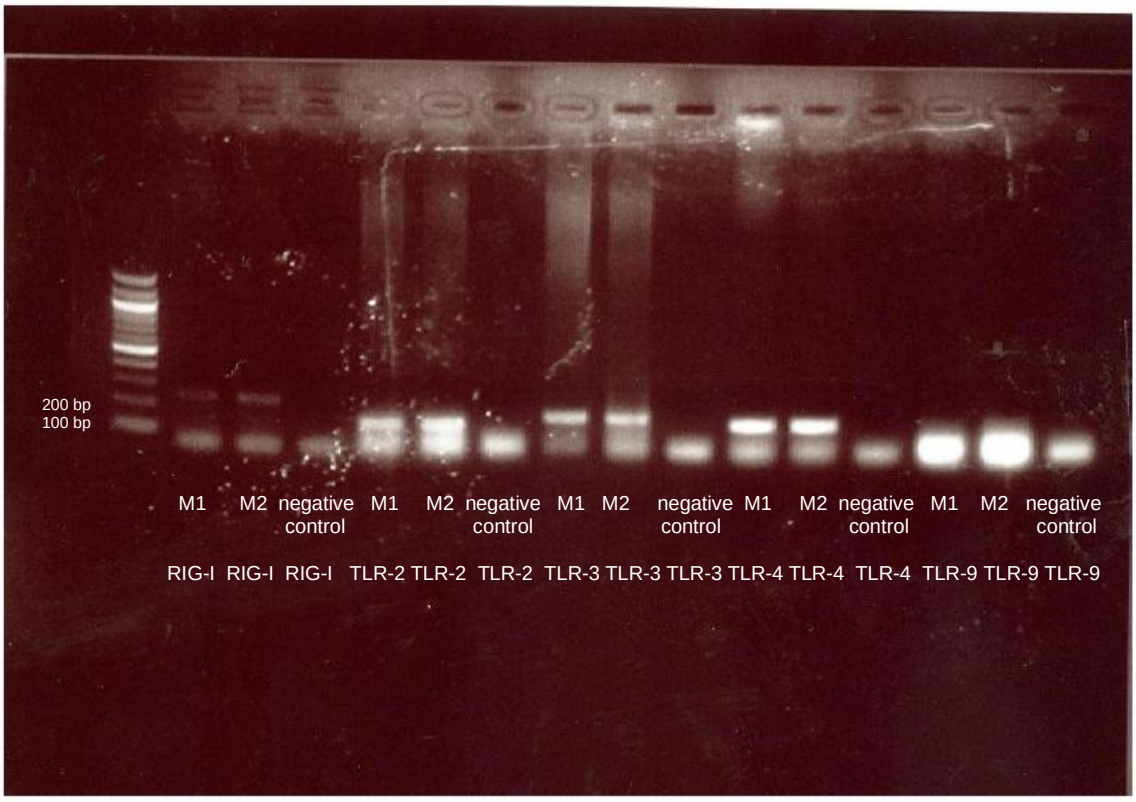

Figure 25: Expression of RIG-I, TLR-2, TLR-3, TLR-4 and TLR-9 in M1-Monocyte-Derived Macrophages (MΦ) (M1), M2-MΦ (M2) and in a negative control, aqua dist., as detected by polymerase chain reaction (PCR). RNA was isolated from M1- and M2-MΦ and retro-transcribed into complementary DNA (cDNA). All products of these reactions were used as template for the PCR reaction with couples of primers complementary for the RIG-I, TLR-2, TLR-3, TLR-4 and TLR-9 gene. As a negative control aqua dist. was used. DNA ladder is run on the left, expected size of the PCR product is 150-200 base pairs (bp).

RNA of each of these four molecules could be shown to be transcribed in M1- as well as M2-MΦ, indicating the presence of these molecules in the cells.

In the case of TLR-9 the situation was less clear. As Figure 25 depicts, putative bands could not be differentiated from primer luminescence and there might not have been any bands at all. This result would be in accordance with reports that limit expression of TLR-9 to plasmacytoid dendritic cells.

3.5.2 Investigation of PML in M1- and M2-MΦ

In order to take a closer look at the presence and fate of PML during HCMV infection, M1- and M2-MΦ were mock- and HCMV-infected (TB40E, moi = 10) for 3, 6 and 24 hours prior to fixation and indirect immunofluorescence staining of PML.

In parallel, one well per MΦ subtype was stained with anti-IE1-2 antibodies in order to assess the infection rates. The typical effect of M2-MΦ being infected to a higher degree than M1-MΦ appeared also for the cells in these experiments.

Over a course of 24 hours a phenomenon was observed that was consistent with the findings on PML during HCMV infection so far. HCMV is able to break PML's structural integrity , thereby probably overcoming the antiviral effects of the ND10 component. [reviewed in 98]

In the beginning of the HCMV infection the amount of nuclear dots indicating PML was more or less the same as in mock infected cells. As infection went on they appeared less numerous and smaller dots, supposedly representing particles from dispersed PML, appeared. This process went on until the majority of PML dots was found as a diffused fluorescence all over the nucleus or the signal for PML was gone completely, presumably indicating that the particles of the dispersed PML had become too small to be detected.

As shown in Figure 26, 3 hours pi green stained dots representing PML within the ND10 complex were still visible in the nuclei of both subtypes of MΦ in the majority of cells and had a compact round shape.

Visible 6 hours pi in M2-MΦ a dissolving process of PML had started. Stained PML dots either appeared in lower number in one section of cells or there were no clearly stained dots visible any more in another. Instead, staining became more unspecific, with a coloring all over the nucleus or very small stained spots that were no longer regarded as PML dots and probably represent dispersed parts of dissolved PML. At the same time, in M1-MΦ, this effect of infection did not yet appear in great numbers.

However, 24 hours pi this changed: In M1-MΦ there were less cells showing staining for PML in their nuclei next to a high number of cells with no signal for PML at all or dispersed PML. In M2-MΦ 24 hours pi, practically all nuclei showed no staining at all or disseminated color all over the nucleus.

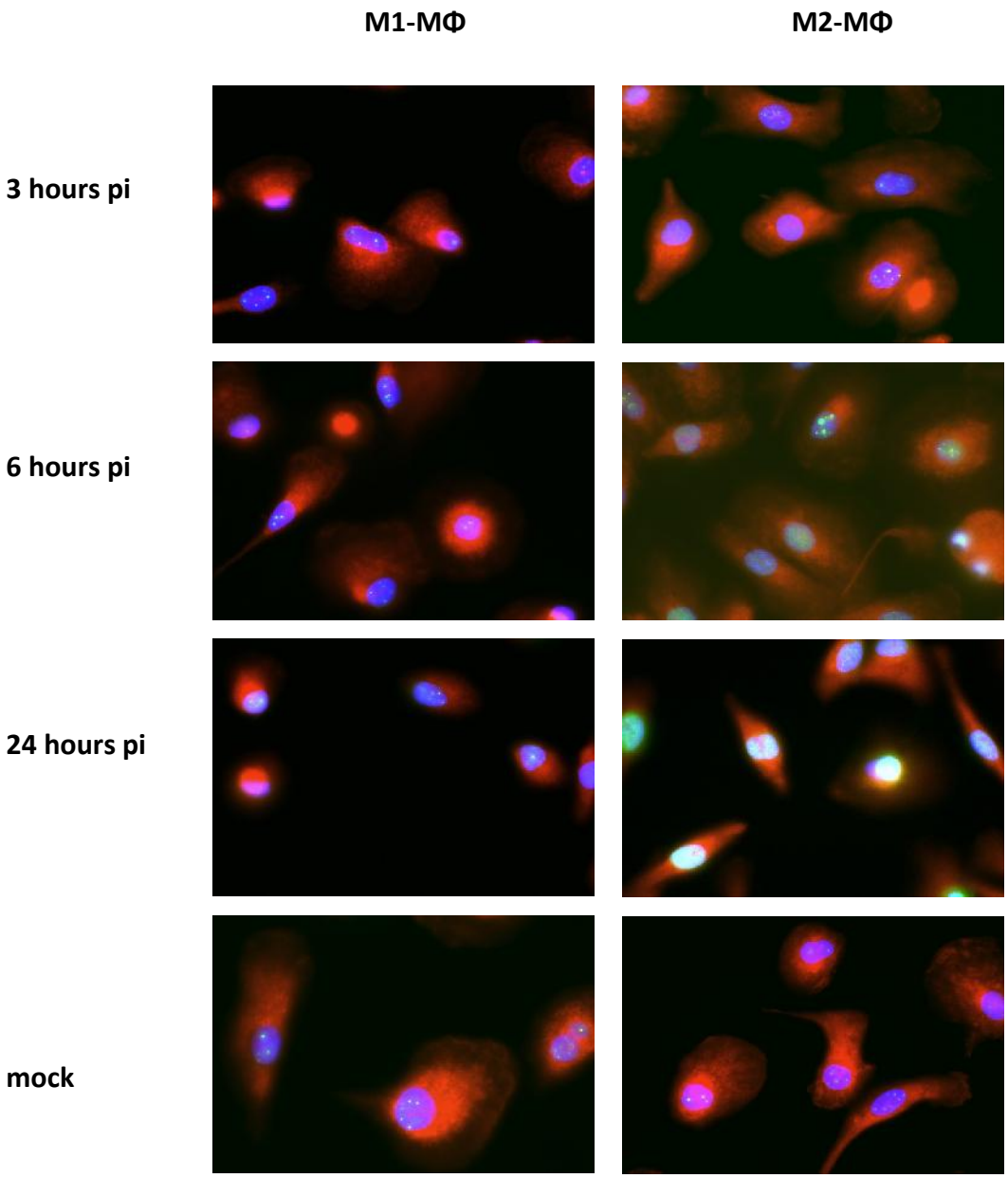

Figure 26: Analysis of promyelocytic leukemia antigen (PML) distribution (green) in M1- and M2-Monocyte-Derived Macrophages (MΦ) during Human cytomegalovirus (HCMV) infection. Cells infected with HCMV strain TB40E with a multiplicity of infection (moi) of 10 for different times (mock, 3, 6 and 24 hours) were incubated with anti-PML antibody and immunofluorescence staining was performed as previously described. This experiment was carried out 3 times, and twice additionally for the mock samples. green: PML, blue: DAPI, red: Evansblue, magnification 63x

So in summary PML apparently is disintegrated in its structure by HCMV earlier and more complete in M2-MΦ than M1-MΦ during the first 24 hours pi.

In order to find out whether there were different basal levels of the immunogenic protein PML in the two MΦ subtypes, M1- and M2-MΦ were compared regarding their expression of PML in an uninfected state. Immunofluorescence single staining for PML was executed as described above. Because PML dispersed into dots by virus infection did not appear under this condition, it was possible to quantify them for big particles of a PML body destroyed by HCMV could not be confused with PML dots.
No conclusive difference could be observed between the two MΦ subsets in the mock state. The mean dot number per cell was 3.93 in M1-MΦ and 3.72 in M2-MΦ.
By performance of student's t-test ($p<0.05$) these rates were found to not be significantly different.

4. Discussion

There are two basic types of macrophages *in vitro*, M1-MΦ and M2-MΦ, generated by stimulation with growth factors GM-CSF or M-CSF respectively. As has been demonstrated in the past [8], M2-MΦ are more susceptible to HCMV infection than M1-MΦ. There are multiple hypotheses to explain this phenomenon during the early events of infection: different cellular expression of HCMV entry receptors, differences in the virus' way from the membrane to the nucleus and dissimilar interaction with intrinsic defensive factors of the cells. In this study, the two cell subsets were compared regarding these factors.

While M1-MΦ are highly immunogenic and pro-inflammatory cells, M2-MΦ are ascribed a tolerogenic and anti-inflammatory potential. This becomes manifest for example in their dissimilar expression of receptors and their ability to produce chemokines and cytokines with opposite functions [reviewed in 64].

Many studies have shown HCMV to bind and use cell surface molecules e.g. CD13 [52,90,91], integrins [29,30,108], BST2/Tetherin [107], EGFR [109] and PDGFR-α [93] as receptors to enter into human cells.

By FACS analysis, it was observed that neither PDGFR-α nor EGFR were expressed on the surface (nor intracellularly) on M1- or M2-MΦ. This was surprising because especially EGFR had been shown to be a receptor used by HCMV to enter into various cell types [108]. On the other hand it should be considered that there is no consensus about the expression of EGFR receptor on hematopoietic cells such as monocytes and macrophages in general [28].

The antibody block of CD13 has been found to prevent HCMV entry into fibroblasts in the past [36,90]. Here, CD13 was found to be expressed in great numbers on the surface of both subtypes of MΦ. However, it seems unlikely that the aminopeptidase is the entry receptor responsible for the dissimilar infection rate of HCMV, for it was not expressed in a dissimilar way on the two MΦ subtypes. This might even question the significance of CD13 as an entry receptor in general, especially as attempts to block the receptor using antibodies failed to decrease infectivity rates. However, the antibody used might not have been reliable since not all reference authors could block HCMV infection following the

same procedure [36]. This problem could perhaps be solved in the future by the use of a different protocol, for example including a lower antibody incubation temperature to exclude cellular internalization of the antibody.

It has to be added that, even though the susceptibility was clearly higher in M2-MΦ than in M1-MΦ in all experiments, the TB40E infectivity measured in these blocking experiments was lower than usually (maybe due to an impaired titer of the virus stock). So, apparently, not even infection with a low viral load was influenced by blocking of CD13.

Similarly, various integrin chains were investigated. A clear cut different expression in distribution or number could not be found on the two cell subsets. In detail, there was a tendency towards a higher expression of integrin chain alpha-X on M2-MΦ than M1-MΦ, but these data need to be confirmed by additional experiments. Furthermore, for the MFI of beta-2 expression there was a weak trend with a stronger signal on M1-MΦ than M2-MΦ.

In conclusion, integrins may work as entry receptors on macrophages. Most of them were clearly expressed. However, it is questionable if they are the crucial factor deciding over the variant infection rates in M1- and M2-MΦ. Especially since there was a high variability between cells obtained from different blood donors, more experiments should be performed in order to verify the detected trends. Also, a wider data set would allow comparison of the expression rates by Student's t-test or similar statistical methods.

Wang and colleagues demonstrated that HCMV uses integrin alphaubeta3 and EGFR as receptor and that the coordination between EGFR and integrin alphaubeta3 (consisting of alpha chain alpha-υ and beta chain beta-3) is essential for HCMV entry [108]. Taking into account the absence of EGFR on MΦ, this might question the role of integrins for HCMV infection in macrophages even more. Indeed, integrin chain beta-3 was, alongside alpha-2b, one of the chains that could not be found on either MΦ. Integrin expression is highly dependent on exposure to proinflammatory agents [11]. Therefore, it might be interesting to reinvestigate integrin chain expression after infection with HCMV in M1- and M2-MΦ.

BST2/Tetherin was proposed to be an entry receptor in fibroblasts and monocytes in 2011 [107]. This surface molecule, usually known as an intrinsic viral restriction factor, was also

detected quantitatively on the surfaces of M1- and M2-MΦ in this study. It was present on both cell types and in all but one experiment there was a higher expression of BST2 on M2-MΦ than M1-MΦ. A closer look at the protein, for example using specific antibodies to block its engagement as performed for CD13 (see above) would be interesting in the future.

After these investigations on the entry of HCMV into M1- and M2-MΦ, the way of viral particles from the cellular membrane to the cellular nucleus was examined. By analyzing two tegument proteins (pp65 and pp150) and one viral surface glycoprotein (gB) it could be shown that the viral translocation to the nucleus takes place faster in M2- as compared to M1-MΦ. As a conclusion, even though the so-far investigated entry receptors do not account for it, a difference seems to exist in the infection course in the two MΦ subsets before the virus reaches the nucleus for replication.

In regard to pp65, it has to be mentioned that it could not be distinguished between its presence in viral particles and in dense bodies or NIEP, which are non-infectious as they represent only isolated structural virus components (but not, for example, DNA).

The interaction of intrinsic factors, i.e. RIG-I, TLRs and PML, to HCMV in the first hours of infection was another aspect of interest.

One hypothesis is that TLRs, important PRRs, could be expressed at higher levels or in a wider range in M1-MΦ than M2-MΦ and thus hamper the infection in M1-MΦ. Especially for TLR-2 there is evidence for a close interaction between the receptor and viral glycoproteins gB and gH leading to an inflammatory antiviral defense [13]. A dissimilar expression of TLR-2 in M1- versus M2-MΦ might therefore lead to an antiviral response of different strength after HCMV infection. The expression of TLR-2, -3, -4 and -9, as well as RIG-I, a molecule with similar functions to TLRs, was evaluated by PCR amplifying the corresponding genes from messenger RNAs. Unfortunately the chosen primers gave rather strong bands under the UV-light themselves thereby somewhat reducing the clarity of the signal of the bands for the sought genes. Also, the expected PCR products, though clearly present for M1- and M2-MΦ, appeared with low intensities. This could not be changed by an increase in RNA amount within the boundaries of this study. Alternatively, a quantification of the transcribed RNA to compare M1- and M2-MΦ should be thought about in the future. So it was difficult to make a clear statement with the

found results. However, during the work on this project, Wu and colleagues investigated by RT-PCR as well as FACS the expression of RIG-I, TLR-3, -7 and -8 and showed that all receptors were present in higher amounts in M2-MΦ, than M1-MΦ [113]. Considering the roles of RIG-I and TLRs in pathogen sensing and anti-viral defenses it could be speculated that HCMV could be less impeded by them in M1-MΦ than in M2-MΦ. This would be in conflict with the higher HCMV infection rates found in M2-MΦ. The experiment should be repeated in a similar way for the receptors examined herein, TLR-2, TLR-4 and TLR-9, including quantification, possibly also by FACS. A method using cDNA dilution row for PCR (used by Schierling *et al.* 2005 [83]) might help here, too. As for TLR-9, the preliminary results herein allow the interpretation that TLR-9 is not expressed in MΦ. This would be in agreement with prior reports describing this receptor as only present in plasmocytoid dendritic cells.

Another cellular anti-viral factor, nuclear protein PML, was examined in order to define its role during HCMV infection in M1- and M2-MΦ. PML has been reported to prevent HCMV IE gene expression directly upon infection. The virus is able to overcome this defense by disintegrating ND10 in its structure and thereby PML. This dispersion of PML that HCMV causes could be seen to take place faster in M2-MΦ than in M1-MΦ. This is a result in agreement with the higher efficiency of infection in this cell subset. Additionally, PML amount was quantified in the two MΦ subtypes prior to infection but PML did not occur in dissimilar amounts in the two MΦ types.

Actually, there is evidence that PML might not be as important in the suppression of HCMV DNA replication as supposed: even in PML knock-down fibroblasts an efficient, presumably cell cycle-dependent, block of HCMV IE gene expression was found after infection [116].

Finally, the possibility was considered that different amounts of viral genome were incorporated in the cellular nucleus in M1- and M2-MΦ. This could have been evaluated quantitatively by fluorescence in situ hybridization (FISH). The method was established for PBMCs, though unfortunately could not be applied to MΦ in the experiments carried out.

In the future, it would be fascinating to learn more about the role of interferons in M1- and M2-MΦ, as there are reports stating that M2-MΦ have a higher basal secretion level

of IFN-β than M1-MΦ [32], while type I interferons are thought to be expressed in M1-MΦ in greater amounts after stimulation with e.g. LPS [64]. There are also reports that HCMV infection might trigger higher IFNɣ secretion in M1-MΦ than in M2-MΦ [8].
Many of the cellular components examined in this study, e.g. BST2 [12], PDGFR-α [68] and PML [98], are IFN-dependent in their expression or are important mediators for expression of type I IFN, like TLR-2 and RIG-I [reviewed in 53]. This raises more questions in the field of a possible dissimilar IFN expression in M1-MΦ and M2-MΦ, as it seemed like there might be a higher expression of BST2 and RIG-I in M2-MΦ.
One could think about how closely the difference in INF- secretion before and after infection should be considered as a possible explanation for the dissimilar susceptibility of M1-MΦ and M2-MΦ to HCMV. If there is a difference in INF secretion and auto-stimulation the corresponding engagement of different cascades leading to immune response could also be dissimilar.
In summary, one definite reason why M1- and M2-MΦ get infected by HCMV in such different amounts, could not be found in this study. Nevertheless, the regarded phases of viral infection, from the entry to the incorporation of the genome, seem to be important to find an answer to this question, as infection is clearly increased in M2-MΦ in comparison to M1-MΦ at this stage already.

5. Summary

Human Cytomegalovirus (HCMV) is a ubiquitous herpesvirus causing high morbidity in individuals with an impaired immune defense. The two major types of monocyte-derived macrophages *in vitro* (MΦ), M1-MΦ and M2-MΦ, are unequally susceptible to infection by HCMV. Anti-inflammatory, anti-immunogenic M2-MΦ get infected about twofold compared to pro-inflammatory, immunogenic M1-MΦ.

In this study differences between the two cell subsets regarding early HCMV infection were examined. The hypothesis in this study was particularly, that dissimilar expression of possible entry receptors or intrinsic restriction factors of viral infection define the different susceptibility.

Indirect immunofluorescence labelling of structural components of the viral tegument and envelope (pp65, pp150 and gB, respectively) showed that already the intracellular translocation of the virus towards the cellular nucleus occurred faster in M2-MΦ than in M1-MΦ.

We investigated whether this was also true for the appearance of viral genomes in cellular nuclei by fluorescence in situ hybridization (FISH). However unfortunately it was not possible to fully establish this method to detect viral DNA in the time frame of this thesis.

Promyelocytic leukemia protein (PML) is an anti-viral nuclear protein that gets disintegrated in its structure by HCMV during infection. Visualization of this destruction process by indirect immunofluorescence staining for the protein showed that it appeared earlier in M2-MΦ than in M1-MΦ, too.

Additionally, PML was quantified using the same method in uninfected M1- and M2-MΦ to detect a putative difference in basal levels of this agent of the immune system. No dissimilarity could be detected thus suggesting that differences in HCMV susceptibility are not due to a higher intrinsic anti-viral activity in the nuclei of M1-MΦ.

Toll- like receptors (TLRs) 2, 3, 4 and 9 and retinoic acid inducible gene I (RIG-I) were investigated in the two cell subsets. This was in order to see if the pathogen recognition receptors (PRRs) differed in their expression and would thus trigger a broader antiviral

response in one cell type than in the other. Qualitatively, TLRs 2, 3, 4 and RIG-1 could be found to be expressed in M1- as well as M2-MΦ by polymerase chain reaction (PCR). Results on TLR-9 were ambiguous but probably showing that it was not expressed.
A range of receptors that had been proposed so far as HCMV entry receptors were investigated by fluorescence activated cell sorting (FACS) analysis in uninfected M1- and M2-MΦ.
Endothelial growth factor receptor (EGFR) and platelet derived growth factor receptor α (PDGFR-α), which were considered so far the main receptors involved during infection of myeloid cells, could not be detected on the surface or intracellularly in M1-MΦ or M2-MΦ.
A broad spectrum of integrin chains was found to be expressed in similar amounts on M1-MΦ and M2-MΦ. In contrast the integrin chains alpha-2b and beta-3, which were the latest to be described as a HCMV receptor, were found to be not expressed at all. Despite the high interdonor variability, for alpha-X a tendency towards a higher expression in M2-MΦ and for could be observed in some experiments.
Surface expression of CD13 was equal on the two cell subsets. Blocking of CD13 by specific antibodies prior infection did not lead to decrease in early viral genome transcription in either M1- or M2-MΦ.
BST expression was higher on M2-MΦ than M1-MΦ in 4 of 5 experiments.
Taken together, none of the examined receptors seems clearly responsible for the difference in HCMV infectivity rates in M1-MΦ and M2-MΦ and a universal role of either of them as entry receptor was questioned. BST2 might be an exception.
In summary, the exact difference between M1- and M2-MΦ explaining their dissimilar susceptibility to HCMV could not be identified in this study. However, it could be shown that especially the early events of infection are worth further investigations to find the explanation to this phenomenon in the future.

6. References

[1] Abate D A, Watanabe S, Mocarski E S: Major human cytomegalovirus structural protein pp65 (ppUL83) prevents interferon response factor 3 activation in the interferon response. J Virol 78: 10995–1006 (2004)

[2] Ahn J, Hayward G: The major immediate-early proteins IE1 and IE2 of human cytomegalovirus colocalize with and disrupt PML-associated nuclear bodies at very early times in infected permissive cells. J Virol 71: 4599–4613 (1997)

[3] Ahn J-H, Hayward G S: Disruption of PML-Associated Nuclear Bodies by IE1 Correlates with Efficient Early Stages of Viral Gene Expression and DNA Replication in Human Cytomegalovirus Infection. Virology 274: 39–55 (2000)

[4] Arnaud F, Black S G, Murphy L, Griffiths D J, Neil S J, Spencer T E, Palmarini M: Interplay between ovine bone marrow stromal cell antigen 2/tetherin and endogenous retroviruses. J Virol 84: 4415–4425 (2010)

[5] Arnon T I, Achdout H, Levi O, Markel G, Saleh N, Katz G, Gazit R, Gonen-Gross T, Hanna J, Nahari E, Porgador A, Honigman A, Plachter B, Mevorach D, Wolf D G, Mandelboim O: Inhibition of the NKp30 activating receptor by pp65 of human cytomegalovirus. Nat Immunol 6: 515–523 (2005)

[6] Arnon T I, Markel G, Mandelboim O: Tumor and viral recognition by natural killer cells receptors. Semin Cancer Biol 16: 348–358 (2006)

[7] AuCoin D P, Smith G B, Meiering C D, Mocarski E S: Betaherpesvirus-conserved cytomegalovirus tegument protein ppUL32 (pp150) controls cytoplasmic events during virion maturation. J Virol 80: 8199–8210 (2006)

[8] Bayer C, Varani S, Wang L, Walther P, Zhou S, Straschewski S, Bachem M, Söderberg-Naucler C, Mertens T, Frascaroli G: Human cytomegalovirus infection of M1 and M2 macrophages triggers inflammation and autologous T-cell proliferation. J Virol 87: 67–79 (2013)

[9] Benacerraf B: A quantitative study of the kinetics of blood clearance of p32-labelled escherichia coli and staphylococci by the reticulo-endothelial system. J Exp Med 110: 27–48 (1959)

[10] Benoit M, Desnues B, Mege J-L: Macrophage polarization in bacterial infections. J Immunol 181: 3733–3739 (2008)

[11] Berton G, Lowell C A: Integrin Signalling in Neutrophils and Macrophages. Cell Signal 11: 621–635 (1999)

[12] Blasius A L, Giurisato E, Cella M, Schreiber R D, Shaw A S, Colonna M: Bone marrow stromal cell antigen 2 is a specific marker of type I IFN-producing cells in the naive mouse, but a promiscuous cell surface antigen following IFN stimulation. J Immunol 177: 3260–3265 (2006)

[13] Boehme K W, Guerrero M, Compton T: Human cytomegalovirus envelope glycoproteins B and H are necessary for TLR2 activation in permissive cells. J Immunol 177: 7094–7102 (2006)

[14] Browne E P, Shenk T: Human cytomegalovirus UL83-coded pp65 virion protein inhibits antiviral gene expression in infected cells. Proc Natl Acad Sci USA 100: 11439–11444 (2003)

[15] Browne E P, Wing B, Coleman D, Shenk T: Altered cellular mRNA levels in human cytomegalovirus-infected fibroblasts: viral block to the accumulation of antiviral mRNAs. J Virol 75: 12319–12330 (2001)

[16] Brunner K T, Hurez D, McCluskey R T, Benacerraf B: Blood clearance of P32-labeled vesicular stomatitis and Newcastle disease viruses by the reticuloendothelial system in mice. J Immunol 85: 99–105 (1960)

[17] Burgess A, Metcalf D: The nature and action of granulocyte-macrophage colony stimulating factors. Blood 56: 947–958 (1980)

[18] Cao S, Liu J, Chesi M, Bergsagel P L, Ho I-C, Donnelly R P, Ma X: Differential regulation of IL-12 and IL-10 gene expression in macrophages by the basic leucine zipper transcription factor c-Maf fibrosarcoma. J Immunol 169: 5715–5725 (2002)

[19] Chan G, Nogalski M T, Yurochko A D: Activation of EGFR on monocytes is required for human cytomegalovirus entry and mediates cellular motility. *Proc Natl Acad Sci USA* 106: 22369–22374 (2009)

[20] Compton T, Kurt-Jones E A, Boehme K W, Belko J, Latz E, Golenbock D T, Finberg R W: Human Cytomegalovirus Activates Inflammatory Cytokine Responses via CD14 and Toll-Like Receptor 2. J Virol 77: 4588–4596 (2003)

[21] Crofton R: The origin, kinetics, and characteristics of the kupffer cells in the normal steady state. J Exp Med 148: 1–17 (1978)

[22] Cuevas-Bennett C, Shenk T: Dynamic histone H3 acetylation and methylation at human cytomegalovirus promoters during replication in fibroblasts. J Virol 82: 9525–9536 (2008)

[23] Delmas B, Gelfi J, Kut E, Sjostrom H, Noren O, Laude H: Determinants essential for the transmissible gastroenteritis virus-receptor interaction reside within a domain of aminopeptidase-N that is distinct from the enzymatic site. J Virol 68: 5216–5224 (1994)

[24] Delmas B, Gelfi J, L'Haridon R, Vogel L K, Sjöström H, Norén O, Laude H: Aminopeptidase N is a major receptor for the entero-pathogenic coronavirus TGEV. Nature 357: 417–420 (1992)

[25] Döhner K, Sodeik B: The role of the cytoskeleton during viral infection. Curr Top Microbiol Immunol 285: 67–108 (2005)

[26] Ellermann-Eriksen S: Macrophages and cytokines in the early defence against herpes simplex virus. Virol J 2: 59 (2005)

[27] Everett R D: Interactions between DNA viruses, ND10 and the DNA damage response. Cell Microbiol 8: 365–374 (2006)

[28] Ewald J A, Wilkinson J C, Guyer C A, Staros J V: Ligand- and kinase activity-independent cell survival mediated by the epidermal growth factor receptor expressed in 32D cells. Exp Cell Res 282: 121–131 (2003)

[29] Feire A L, Koss H, Compton T: Cellular integrins function as entry receptors for human cytomegalovirus via a highly conserved disintegrin-like domain. Proc Natl Acad Sci USA 101: 15470–15475 (2004)

[30] Feire A L, Roy R M, Manley K, Compton T: The glycoprotein B disintegrin-like domain binds beta 1 integrin to mediate cytomegalovirus entry. J Virol 84: 10026–10037 (2010)

[31] Fish K, Depto A, Moses A, Britt W, Nelson J: Growth kinetics of human cytomegalovirus are altered in monocyte- derived macrophages. J Virol 69: 3737–3743 (1995)

[32] Fleetwood A J, Dinh H, Cook A D, Hertzog P J, Hamilton J A: GM-CSF- and M-CSF-dependent macrophage phenotypes display differential dependence on type I interferon signaling. J Leukoc Biol 86: 411–421 (2009)

[33] Fleetwood A J, Lawrence T, Hamilton J A, Cook A D: Granulocyte-macrophage colony-stimulating factor (CSF) and macrophage CSF-dependent macrophage phenotypes display differences in cytokine profiles and transcription factor activities: implications for CSF blockade in inflammation. J Immunol 178: 5245–5252 (2007)

[34] Fong C H Y, Bebien M, Didierlaurent A, Nebauer R, Hussell T, Broide D, Karin M, Lawrence T: An antiinflammatory role for IKKbeta through the inhibition of 'classical' macrophage activation. J Exp Med 205: 1269–1276 (2008)

[35] Gilbert M J, Riddell S R, Plachter B, Greenberg P D: Cytomegalovirus selectively blocks antigen processing and presentation of its immediate-early gene product. Nature 383: 720–722 (1996)

[36] Giugni T D, Soderberg C, Ham D J, Bautista R M, Hedlund K-O, Moller E, Zaia J A: Neutralization of Human Cytomegalovirus by Human CD13-Specific Antibodies. J Infect Dis 173: 1062–1071 (1996)

[37] Gordon S: Alternative activation of macrophages. Nat Rev Immunol 3: 23–35 (2003)

[38] Groom H C T, Yap M W, Galão R P, Neil S J D, Bishop K N: Susceptibility of xenotropic murine leukemia virus-related virus (XMRV) to retroviral restriction factors. Proc Natl Acad Sci USA. 107: 5166–5171 (2010)

[39] Groves I J, Reeves M B, Sinclair J H: Lytic infection of permissive cells with human cytomegalovirus is regulated by an intrinsic 'pre-immediate-early' repression of viral gene expression mediated by histone post-translational modification. J Gen Virol 90: 2364–2374 (2009)

[40] Hamilton J A: Colony-stimulating factors in inflammation and autoimmunity. Nat Rev Immunol 8: 533–544 (2008)

[41] Hobom U, Brune W, Messerle M, Hahn G, Koszinowski U H: Fast screening procedures for random transposon libraries of cloned herpesvirus genomes: mutational analysis of human cytomegalovirus envelope glycoprotein genes. J Virol 74: 7720–7729 (2000)

[42] Hume D A: Macrophages as APC and the dendritic cell myth. J Immunol 181: 5829–5835 (2008)

[43] Isaacson M K, Compton T: Human cytomegalovirus glycoprotein B is required for virus entry and cell-to-cell spread but not for virion attachment, assembly, or egress. J Virol 83: 3891–3903 (2009)

[44] Isaacson M K, Feire A L, Compton T: Epidermal growth factor receptor is not required for human cytomegalovirus entry or signaling. *J Virol* 81: 6241–6247 (2007)

[45] Ishov A M: Human Cytomegalovirus Immediate Early Interaction with Host Nuclear Structures: Definition of an Immediate Transcript Environment. J Cell Biol 138: 5–16 (1997)

[46] Ishov A M: PML Is Critical for ND10 Formation and Recruits the PML-interacting Protein Daxx to this Nuclear Structure When Modified by SUMO-1. J Cell Biol 147: 221–234 (1999)

[47] Johnson R A, Wang X, Ma X L, Huong S M, Huang E S: Human cytomegalovirus up-regulates the phosphatidylinositol 3-kinase (PI3-K) pathway: inhibition of PI3-K activity inhibits viral replication and virus-induced signaling. J Virol 75:6022–6032 (2001)

[48] N. Jouvenet N, Neil S J D, Zhadina M, Zang T, Kratovac Z, Lee Y, McNatt M, Hatziioannou T, Bieniasz P D: Broad-spectrum inhibition of retroviral and filoviral particle release by tetherin. J Virol 83: 1837–1844 (2009)

[49] Kalejta R F: Tegument proteins of human cytomegalovirus. Microbiol Mol Biol Rev 72: 249–265 (2008)

[50] Kalejta R F, Shenk T: Proteasome-dependent, ubiquitin-independent degradation of the Rb family of tumor suppressors by the human cytomegalovirus pp71 protein. Proc Natl Acad Sci USA 100: 3263–3268 (2003)

[51] Kaletsky R L, Francica J R, Agrawal-Gamse C, Bates P: Tetherin-mediated restriction of filovirus budding is antagonized by the Ebola glycoprotein. Proc Natl Acad Sci USA 106: 2886–2891 (2009)

[52] KasmanL M: CD13/aminopeptidase N and murine cytomegalovirus infection. Virology 334: 1–9 (2005)

[53] Kawai T, Akira S: Toll-like receptor and RIG-I-like receptor signaling. Ann NY Acad Sci 1143: 1–20 (2008)

[54] Kowalik T F, Wing B, Haskill J S, Azizkhan J C, Baldwin A S, Huang E S: Multiple mechanisms are implicated in the regulation of NF-kappa B activity during human cytomegalovirus infection. Proc Natl Acad Sci 90: 1107–1111 (1993)

[55] Krausgruber T, Blazek K, Smallie T, Alzabin S, Lockstone H, Sahgal N, Hussell T, Feldmann M, Udalova I A: IRF5 promotes inflammatory macrophage polarization and TH1-TH17 responses. Nat Immunol 12: 231–238 (2011)

[56] Kupzig S, Korolchuk V, Rollason R, Sugden A, Wilde A, Banting G: Bst-2/HM1.24 Is a Raft-Associated Apical Membrane Protein with an Unusual Topology. Traffic 4: 694–709 (2003)

[57] Laskin D L, Weinberger B, Laskin J D: Functional heterogeneity in liver and lung macrophages. J Leukoc Biol 70: 163–170 (2001)

[58] Le Tortorec A, Neil S J D: Antagonism to and intracellular sequestration of human tetherin by the human immunodeficiency virus type 2 envelope glycoprotein. J Virol 83: 11966–11978 (2009)

[59] Lieberman P M, Sinclair J: Chromatin structure regulates human cytomegalovirus gene expression during latency, reactivation and lytic infection. Biochim Biophys Acta - Gene Regul Mech 1799: 286–295 (2010)

[60] Look A T, Ashmun R A, Shapiro L H, Peiper S C: Human myeloid plasma membrane glycoprotein CD13 (gp150) is identical to aminopeptidase N. J Clin Invest 83: 1299–1307 (1989)

[61] MacKinnon A C, Farnworth S L, Hodkinson P S, Henderson N C, Atkinson K M, Leffler H, Nilsson U J, Haslett C, Forbes S J, Sethi T: Regulation of alternative macrophage activation by galectin-3. J Immunol 180: 2650–2658 (2008)

[62] Mansouri M, Viswanathan K, Douglas J L, Hines J, Gustin J, Moses A V, Früh K: Molecular mechanism of BST2/tetherin downregulation by K5/MIR2 of Kaposi's sarcoma-associated herpesvirus. J Virol 83: 9672–9681 (2009)

[63] Mantovani A, Sica A, Sozzani S, Allavena P, Vecchi A, Locati M: The chemokine system in diverse forms of macrophage activation and polarization. Trends Immunol 25: 677–686 (2004)

[64] Mantovani A, Sozzani S, Locati M, Allavena P, Sica A: Macrophage polarization: tumor-associated macrophages as a paradigm for polarized M2 mononuclear phagocytes. Trends Immunol 23: 549–555 (2002)

[65] McLaughlin-Taylor E, Pande H, Forman S J, Tanamachi B, Li C R, Zaia J A, Greenberg P D, Riddell S R: Identification of the major late human cytomegalovirus matrix protein pp65 as a target antigen for CD8+ virus-specific cytotoxic T lymphocyte*s. J* Med Virol 43: 103–110 (1994)

[66] Michelson S: Interaction of human cytomegalovirus with monocytes/macrophages: a love-hate relationship. Pathol Biol (Paris) 45: 146–158 (1997)

[67] Mocarski P R F, Edward S, Shenk T: Cytomegaloviruses. In: Fields Virology, 5th ed., vol. 2, P. M. Knipe, D.M.; Howley Ed., Wolters Kluwer Health Lippincott Williams & Wilkins, pp. 2701–2772 (2007)

[68] Morelli P I, Martinsson S, Ostergren-Lundén G, Fridén V, Moses J, Bondjers G, Krettek A, Lustig F: IFNgamma regulates PDGF-receptor alpha expression in macrophages, THP-1 cells, and arterial smooth muscle cells. Atherosclerosis 184: 39–47 (2006)

[69] Mosser D M, Edwards J P: Exploring the full spectrum of macrophage activation. Nat Rev Immunol 8: 958–969 (2008)

[70] Munger J, Yu D, Shenk T: UL26-deficient human cytomegalovirus produces virions with hypophosphorylated pp28 tegument protein that is unstable within newly infected cells. J Virol 80: 3541–3548 (2006)

[71] Murray P J, Wynn T A: Protective and pathogenic functions of macrophage subsets. Nat Rev Immunol 11: 723–237 (2011)

[72] Odeberg J, Plachter B, Brandén L, Söderberg-Nauclér C: Human cytomegalovirus protein pp65 mediates accumulation of HLA-DR in lysosomes and destruction of the HLA-DR alpha-chain. Blood 101: 4870–4877 (2003)

[73] Pardieu C, Vigan R, Wilson S J, Calvi A, Zang T, Bieniasz P, Kellam P, Towers G J, Neil S J D: The RING-CH ligase K5 antagonizes restriction of KSHV and HIV-1 particle release by mediating ubiquitin-dependent endosomal degradation of tetherin. PLoS Pathog 6, e1000843 (2010)

[74] Paulus C, Krauss S, Nevels M: A human cytomegalovirus antagonist of type I IFN-dependent signal transducer and activator of transcription signaling. Proc Natl Acad Sci USA 103: 3840–3845 (2006)

[75] Penfold M E T, Mocarski E S: Formation of Cytomegalovirus DNA Replication Compartments Defined by Localization of Viral Proteins and DNA Synthesis. Virology 239: 46–61 (1997)

[76] Radoshitzky S R, Dong L, Chi X, Clester J C, Retterer C, Spurgers K, Kuhn J H, Sandwick S, Ruthel G, Kota K, Boltz D, Warren T, Kranzusch P J, Whelan S P J, Bavari S: Infectious Lassa virus, but not filoviruses, is restricted by BST-2/tetherin. J Virol 84: 10569–10580 (2010)

[77] Reboredo M, Greaves R F, Hahn G: Human cytomegalovirus proteins encoded by UL37 exon 1 protect infected fibroblasts against virus-induced apoptosis and are required for efficient virus replication. J Gen Virol 85: 3555–3567 (2004)

[78] Reeves M B, MacAry P A, Lehner P J, Sissons J G P, Sinclair J H: Latency, chromatin remodeling, and reactivation of human cytomegalovirus in the dendritic cells of healthy carriers. Proc Natl Acad Sci U*SA* 102: 4140–4145 (2005)

[79] Rossini G, Cerboni C, Santoni A, Landini M P, Landolfo S, Gatti D, Gribaudo G, Varani S: Interplay between human cytomegalovirus and intrinsic/innate host responses: a complex bidirectional relationship. Mediators Inflamm 2012: 607276 (2012)

[80] Ryckman B J, Jarvis M A, Drummond D D, Nelson J A, Johnson D C: Human cytomegalovirus entry into epithelial and endothelial cells depends on genes UL128 to UL150 and occurs by endocytosis and low-pH fusion. J Virol 80: 710–722 (2006)

[81] Sakuma T, Noda T, Urata S, Kawaoka Y, Yasuda J: Inhibition of Lassa and Marburg virus production by tetherin. J Virol 83: 2382–2385 (2009)

[82] Sampaio K L, Cavignac Y, Stierhof Y-D, Sinzger C: Human cytomegalovirus labeled with green fluorescent protein for live analysis of intracellular particle movements. J Virol 79: 2754–2767 (2005)

[83] Schierling K, Buser C, Mertens T, and M. Winkler M: Human cytomegalovirus tegument protein ppUL35 is important for viral replication and particle formation. J Virol 79: 3084–3096 (2005)

[84] Scott I: Degradation of RIG-I following cytomegalovirus infection is independent of apoptosis. Microbes Infect 11: 973–979 (2009)

[85] Semenza G: Anchoring and biosynthesis of stalked brush border membrane proteins: glycosidases and peptidases of enterocytes and renal tubuli. Annu Rev Cell Biol 2: 255–313 (1986)

[86] Simmen K A, Singh J, Luukkonen B G, Lopper M, Bittner A, Miller N E, Jackson M R, Compton T, Früh K: Global modulation of cellular transcription by human cytomegalovirus is initiated by viral glycoprotein B. Proc Natl Acad Sci USA 98: 7140–7145 (2001)

[87] Sinclair J, Sissons P: Latent and Persistent Infections of Monocytes and Macrophages. Intervirology 39: 293–301 (1996)

[88] Sinzger C, Digel M, Jahn G: Cytomegalovirus cell tropism. Curr Top Microbiol Immunol 325: 63–83 (2008)

[89] Skaletskaya A, Bartle L M, Chittenden T, McCormick A L, Mocarski E S, Goldmacher V S: A cytomegalovirus-encoded inhibitor of apoptosis that suppresses caspase-8 activation. Proc Natl Acad Sci USA 98: 7829–7834 (2001)

[90] Soderberg C, Giugni T D, Zaia J A, Larsson S, Wahlberg J M, Moller E: CD13 (human aminopeptidase N) mediates human cytomegalovirus infection. J Virol 67: 6576–6585 (1993)

[91] Soderberg C, Larsson S, Bergstedt-Lindqvist S, Moller E: Definition of a subset of human peripheral blood mononuclear cells that are permissive to human cytomegalovirus infection. J Virol 67: 3166–3175 (1993)

[92] Söderberg-Nauclér C, Streblow D N, Fish K N, Allan-Yorke J, Smith P P, Nelson J A: Reactivation of latent human cytomegalovirus in CD14(+) monocytes is differentiation dependent. J Virol 75: 7543–7554 (2001)

[93] Soroceanu L, Akhavan A, Cobbs C S: Platelet-derived growth factor-alpha receptor activation is required for human cytomegalovirus infection. Nature 455: 391–395 (2008)

[94] Stadler M, Chelbi-Alix M K, Koken M H, Venturini L, Lee C, Saïb A, Quignon F, Pelicano L, Guillemin M C, Schindler C: Transcriptional induction of the PML growth suppressor gene by interferons is mediated through an ISRE and a GAS element. Oncogene 11: 2565–2573 (1995)

[95] Stefater J A, Ren S, Lang R A, Duffield J S: Metchnikoff's policemen: macrophages in development, homeostasis and regeneration. Trends Mol Med 17: 743–752 (2011)

[96] Tandon R, Mocarski E S: Control of cytoplasmic maturation events by cytomegalovirus tegument protein pp150. J Virol 82: 9433–9444 (2008)

[97] Tavalai N, Papior P, Rechter S, Leis M, Stamminger T: Evidence for a role of the cellular ND10 protein PML in mediating intrinsic immunity against human cytomegalovirus infections. J Virol 80: 8006–8018 (2006)

[98] Tavalai N, Stamminger T: Interplay between Herpesvirus Infection and Host Defense by PML Nuclear Bodies. Viruses 1: 1240–1264 (2009)

[99] Taylor R T Bresnahan W A: Human cytomegalovirus immediate-early 2 protein IE86 blocks virus-induced chemokine expression. J Virol 80: 920–928 (2006)

[100] Torok D, Ching R W, Bazett-Jones D P: PML nuclear bodies as sites of epigenetic regulation. Front Biosci (Landmark Ed) 14: 1325–1336 (2009)

[101] Valyi-Nagy T, Bandi Z, Boldogh I, Albrecht T: Hydrolysis of inositol lipids: an early signal of human cytomegalovirus infection. Arch Virol 101: 199–207 (1988)

[102] R. van Furth: The origin and kinetics of mononuclear phagocytes. J Exp Med 128: 415–435 (1968)

[103] R. Van Furth: Quantitative study on the production and kinetics of mononuclear phagocytes during an acute inflammatory reaction. J Exp Med 138: 1314–1330 (1973)

[104] Vanarsdall A L, Wisner T W, Lei H, Kazlauskas A, Johnson D C: PDGF receptor-α does not promote HCMV entry into epithelial and endothelial cells but increased quantities stimulate entry by an abnormal pathway. PLoS Pathog: e1002905 (2012)

[105] Verreck F A W, de Boer T, Langenberg D M L, Hoeve M A, Kramer M, Vaisberg E, Kastelein R, Kolk A, de Waal-Malefyt R, Ottenhoff T H M: Human IL-23-producing type 1 macrophages promote but IL-10-producing type 2 macrophages subvert immunity to (myco)bacteria. Proc Natl Acad Sci USA 101: 4560–4565 (2004)

[106] Verreck F A W, de Boer T, Langenberg D M L, van der Zanden L, Ottenhoff T H M: Phenotypic and functional profiling of human proinflammatory type-1 and anti-inflammatory type-2 macrophages in response to microbial antigens and IFN-gamma- and CD40L-mediated costimulation. J Leukoc Biol 79: 285–293 (2006)

[107] Viswanathan K, Smith M S, Malouli D, Mansouri M, Nelson J A, Früh K: BST2/Tetherin enhances entry of human cytomegalovirus. PLoS Pathog 7: e1002332 (2011)

[108] Wang X, Huang D Y, Huong S-M, and E.-S. Huang: Integrin alphavbeta3 is a coreceptor for human cytomegalovirus. Nat Med 11: 515–521 (2005)

[109] Wang X H E, Huong S, Chiu M, Raab-Traub N: Epidermal growth factor receptor is a cellular receptor for human cytomegalovirus. Nature 424: 456–461 (2003)

[110] Weidner J M, Jiang D, Pan X-B, Chang J, Block T M, Guo J-T: Interferon-induced cell membrane proteins, IFITM3 and tetherin, inhibit vesicular stomatitis virus infection via distinct mechanisms. J Virol 84: 12646–12657 (2010)

[111] Wiebusch L: Human cytomegalovirus immediate-early over protein 2 (IE2)-mediated activation of cyclin E is cell-cycle-independent and forces S-phase entry in IE2-arrested cells. J Gen Virol 84: 51–60 (2003)

[112] Wiebusch L, Hagemeier C: The human cytomegalovirus immediate early 2 protein dissociates cellular DNA synthesis from cyclin-dependent kinase activation. EMBO J 20: 1086–1098 (2001)

[113] Wu M-F, Chen S-T, Yang A-H, Lin W-W, Lin Y-L, Chen N-J, Tsai I-S, Li L, Hsieh S-L: CLEC5A is critical for dengue virus-induced inflammasome activation in human macrophages. Blood 121: 95–106 (2013)

[114] Yeager C L, Ashmun R A, Williams R K, Cardellichio C B, Shapiro L H, Look A T, Holmes K V: Human aminopeptidase N is a receptor for human coronavirus 229E. Nature 357: 420–422 (1992)

[115] Zhong S, Muller S, Ronchetti S, Freemont P S, Dejean A, Pandolfi P P: Role of SUMO-1-modified PML in nuclear body formation. Blood 95: 2748–2752 (2000)

[116] Zydek M, Uecker R, Tavalai N, Stamminger T, Hagemeier C, Wiebusch L: General blockade of human cytomegalovirus immediate-early mRNA expression in the S/G2 phase by a nuclear, Daxx- and PML-independent mechanism. J Gen Virol 92: 2757–2769 (2011)

Acknowledgements

I would like to thank Prof. Thomas Mertens for his support of my work in his institute, where I had the opportunity to learn inestimably interesting lessons about science and meet exceptional people.

I thank my supervisor, Dr. Giada Frascaroli, for her constant help and support, patience, intelligent advise and unbreakable optimism, and for being a (female) role model.

Thanks to everyone I had the honor to work with during my time in the laboratory, the members of my working group Carina Bayer, Corinna Setz, Jutta Hegler, Andrea Bauer, Steffen Eipper, Tatjana Schmal and Carolin Tauber for their help and for their humor and kindness.

I thank all the colleagues from the other groups, Dr. Jens von Einem, especially for the help with my PCR experiments, Prof. Christian Sinzger and Dr. Barbara Reinhardt for their precious career advice.

Thanks to Ingrid Bennett, Anke Lüske and Thomas Schmid for being the persons you could always go to for help.

I thank my friends.

I thank my family for everything, including roasting lamb on a spit in the front yard.

Curriculum Vitae

Name	Franziska Radtke
Address	Kurze Lemppen 2
	89075 Ulm
Phone	015124186295
Email	franziska.radtke@uni-ulm.de
Date of birth	15th of june 1990
Place of birth	Munich

Education

10/2009-present	Ulm University, Course of studies: medicine
04/2015	Zweiter Abschnitt der Ärztlichen Prüfung
09/2014	Institute of Physiology, University of Concepción, Chile, Scientific exchange program
09/2012-10/2013	Institute of Virology, University Hospital Ulm, Work on Dissertation in Medicine
09/2011	Erster Abschnitt der Ärztlichen Prüfung
09/2000-06/2009	Karolinen-Gymnasium, School leaving certificate: Abitur

Clinical practice

08/2009, 03/2010, 08/2010	Romed Klinikum Rosenheim Nursing (internship)
03/2012	Pediatric Clinic, Romed Klinikum Rosenheim Clinical traineeship
08/2012	Nervenärztliche Gemeinschaftspraxis Ulm; Dr. Lang Clinical traineeship
08/2013	University Hospital Ulm Clinic for Internal Medicine III Clinical traineeship
03/2014	University Hospital Ulm Clinic for Pediatric Psychiatry Clinical Traineeship

Language Skills

English	7 years of class, good
French	6 years of class (intensive course), good
Spanish	3 years of class, basic knowledge
German	Native language

Methodical Skills

Cell culture; cultivation, concentration, purification and titration of human pathogenic virus; indirect immunofluorescence, fluorescence activated cell sorting (FACS), fluorescence in-situ hybridization (FISH), RNA-extraction, RT-PCR, PCR, Western-blot.

Additional information

Voluntary work	Hochschulgruppe BUND (Bund für Umwelt und Naturschutz Deutschland), Ulm University
Interests	Reading, Traveling, Astronomy, Nature, Art